Design of meta-heuristic computing paradigms for Hammerstein identification systems in electrically stimulated muscle models

Ammara Mehmood[1], Aneela Zameer[2], Naveed Ishtiaq Chaudhary[3], Sai Ho Ling[4, #], Muhammad Asif Zahoor Raja[5]

[1]Department of Electrical Engineering, Pakistan Institute of Engineering and Applied Sciences, Nilore, Islamabad, Pakistan
ms_mehmud16@pieas.edu.pk;

[2]Department of Computer and Information Sciences, Pakistan Institute of Engineering and Applied Sciences, Nilore, Islamabad, Pakistan
aneelaz@pieas.edu.pk

[3]Department of Electrical Engineering, International Islamic University, Islamabad, Pakistan
naveed.ishtiaq@iiu.edu.pk

[4]School of Biomedical Engineering, Centre for Health Technologies, Department of Engineering and IT, University of Technology, Sydney, NSW, Australia
Steve.Ling@uts.edu.au
[#]Corresponding author

[3]Department of Electrical and Computer Engineering, COMSATS University Islamabad, Attock Campus, Attock, Pakistan
muhammad.asif@ciit-attock.edu.pk

Abstract: In this study, a novel application of differential evolution (DE) based computational heuristics is proposed for identification of Hammerstein structures representing the electrically stimulated muscle (ESM) models as a part of rehabilitation interventions for the stock patient to prevent the post spinal cord injury atrophy. The strength of approximation theory is incorporated for defining the fitness function for ESM system based on mean square deviation between actual and estimated responses. DE, genetic algorithms (GAs), particle swarm optimization (PSO), pattern search (PS) and simulated annealing (SA) are used as optimization mechanisms to identify the ESM models with input nonlinearities of sigmoidal, polynomial and spline kernels for noiseless and noisy environments. Comparative studies based on detailed statistics establish the worth of DE based heuristics over its counterparts GAs, PSO, PS and SA in terms of accuracy, convergence, robustness and efficiency for identification of ESM models arising in rehabilitation of the stock patients.

Keywords: Parameter Estimation; Electrically Stimulated Muscle Models; Differential Evolution; Genetic Algorithms; Nonlinear Hammerstein Systems; Evolutionary Computing.

1. Introduction

The spinal cord injury (SCI) has significant impact on volitional activities of muscle and may effect in reducing the cross-sectional area of the muscle nearly by 45% during the first few weeks of SCI [1]. The individuals suffering from SCI are more at the risk of lifetime than non-SCI patients

[2]. Rehabilitation interventions are essential for prevention of post SCI atrophy in order to enhance the effectiveness of muscle strength. Electrical muscle stimulation is a viable post SCI strategy with objective to trigger muscle hypertrophy for enhancing density of muscle with respect to its healthy level and accordingly improves torque output and combats fatigue [3-4]. Electrical muscle stimulation is also helpful in restoration of routine functions such as stretching, bending and reaching [5].

Design of controllers is required to facilitate the application of electrical stimulation for rehabilitation of stroke patients with accurate modeling of electrically stimulated muscle (ESM). Modeling of ESM has been a challenging task and research community has paid special attention to model muscle dynamics, considering both isometric and non-isometric conditions. These models are categorized into Hill-type [6], mathematical [7-8], and block oriented Hammerstein-Wiener structures [9-10]. After detailed experimentations carried out at the rehabilitation center, Southampton University, it was determined that nonlinear Hammerstein system best describes the muscle activation system having a well-defined structure and different estimation techniques for each block [11]. Hammerstein structure comprises of two blocks; first part represents nonlinear systems while subsequent block for linear characteristics [12-13]. In relation to the ESM model, static nonlinearity characterizes the isometric recruitment curve which is a gain relation between the activation levels of the stimulus and output torque, assuming the fixed length of the muscle [12]. While the linear block represents ESM contraction dynamics that combines with isometric recruitment curve to produce average torque [12]. After accurate modeling, the next phase is the parameter estimation of Hammerstein system representing the ESM model.

Researchers have great contributions to develop reliable mechanisms for identification of Hammerstein models [14-16] including, modified gradient descent and recursive least squares strategies incorporating hierarchical approach [17-18]. Furthermore, multi innovation method [19-20], auxiliary mechanism [21] and parameter separation theory [22] have also been proposed. In the recent years, fractional order gradient schemes were effectively employed for parameter identification of nonlinear Hammerstein models [23-28]. These all are deterministic procedures with their own advantages, applications, and limitations while the stochastic techniques [29-34] are not extensively exploited for the parameter estimation of input nonlinear Hammerstein systems as yet. Few potential applications of these methodologies based on exploration and exploitation of artificial neural networks (ANNs), differential evolution (DE) and genetic algorithms (GAs) include fractional order systems [35-36], nonlinear singularly perturb systems [37], nonlinear pantograph systems [38], nonlinear prey–predator models [39], nonlinear chaotic systems [40-41], models of nonlinear optics [42], random matrix theory based application [43], thin film flow systems [44], thermal analysis of porous fin model [45], input nonlinear control autoregressive systems [46-47], active noise control systems [48-49] and control autoregressive moving average systems [50]. Beside these recently stochastic solvers are used to address viably the optimization problems arising in various domains such as astrophysics [51-52], atomic physics [53-54], plasma physics [55-56], thermodynamics [57], mechanics [58-59], nanotechnology [60-61], electric circuits [62-63], energy [64-65], power [66-67], finance [68-69], economics [70-71] and bioinformatics [72-73]. These are the motivational aspects for authors to investigate in the domain of parameter estimation of input nonlinear Hammerstein system representing the electrically stimulated muscle model scenarios through DE, GAs and particle swarm optimization (PSO) as global search mechanisms, as well as pattern search (PS) and simulated annealing (SA).

The salient features of the research study are briefly presented as follows:

- Novel exploitation of computational heuristics through differential evolution in the field of biomedical signal processing to estimate the parameters of electrically stimulated muscle model for rehabilitation of stroke patients.
- Hammerstein structure based ESM model with cubic-spline, sigmoid, and polynomial nonlinearities in the dynamics are effectively identified with respect to true parameters of the system.
- The performance of DE based scheme in terms of accuracy, stability and robustness is invariably better from GAs, PSO, PS and SA for noiseless as well as low and high noisy scenarios of all examples of ESM models.
- The consistency of the worthy identification of differential evolution is indorsed through statistical observations on multiple trails by means of precision and complexity indices.

Organization of paper is as follows: the designed methodology in the form of mathematical formulation for the ESM model and its optimization methodology based on DE and GAs is presented in Section II, in Section III performance indices are narrated in details, in Section IV statistical analyses on large dataset is presented, while in the last Section a brief list of conclusions is provided.

2. Design methodology

The design procedure is presented here that consist of two phases; in the first phase, an overview of electrically stimulated muscle (ESM) models along with formulation of objective function is given, while in the second phase, a brief overview of the optimization solver based on DE and GAs is provided for parameter identification problem of ESM. The schematic of workflow proposed in the present study is illustrated in Fig. 1.

2.1 Electrically stimulated muscle modelling

The modeling of ESM dynamics is carried out through a nonlinear Hammerstein structure in discrete-time is shown in Fig. 2, and is mathematically written as [11-13].

$$x(t)=\frac{P(z)}{Q(z)}g\left(u(t)\right)+\frac{1}{Q(z)}n(t), \tag{1}$$

Here, $u(t)$ represents stimulation input, $x(t)$ denotes system output and $n(t)$ stands for disturbance noise. $P(z)$ is the polynomial defining poles, while $Q(z)$ is the polynomials representing zeros:

$$P(z)=p_1z^{-1}+p_2z^{-2}+\cdots+p_{n_p}z^{-n_p}, \tag{2}$$

$$Q(z)=1+q_1z^{-1}+q_2z^{-2}+\cdots+q_{n_q}z^{-n_q}. \tag{3}$$

Activation function representing nonlinear system input of muscle dynamics is $g(u)$. $g(u)$ for polynomial nature of input is expressed as:

$$g(u)=\gamma_1u+\gamma_2u^2+\gamma_3u^3+\cdots+\gamma_mu^m. \tag{4}$$

Here, $\gamma_1, \gamma_2, \gamma_3, \cdots, \gamma_m$ are coefficients of polynomial and m is the degree of the polynomial.

In higher order derivative system might be at risk of oscillations. Another option is spline function but their derivatives are not continuous at their break points or knots. So, cubic spline is used to model the nonlinear block. Additionally, sigmoid functions are good alternatives. Here, $f(u)$ for sigmoid and cubic-spline nature of input are expressed as: [11]:

$$g(u) = \gamma_1 . \frac{e^{\gamma_2 u} - 1}{e^{\gamma_2 u} + \gamma_3}, \tag{5}$$

$$g(u) = \sum_{i=1}^{m-2} \gamma_i \left| u - u_{i+1} \right|^3 + \gamma_{m-1} + \gamma_m u + \gamma_{m+1} u^2 + \gamma_{m+2} u^3 \tag{6}$$

Taking one knot at 150 in the cubic-spline activation function, equation (6) takes the form:

$$g(u) = \gamma_1 \left| u - 150 \right|^3 + \gamma_2 + \gamma_3 u + \gamma_4 u^2 + \gamma_5 u^3, \tag{7}$$

In order to define the cost function, let define the true parameter vector of ESM model is

$$\vartheta = \left[\vartheta_l, \vartheta_n \right], \tag{8}$$

here ϑ_l represents parameter for linear and ϑ_n for nonlinear blocks of ESM model, respectively. ϑ_l is described as:

$$\vartheta_l = \left[q_1, q_2, ..., q_{n_q}, p_1, p_2, ..., p_{n_p} \right], \tag{9}$$

The parameters related to nonlinear block are denoted by ϑ_n and by assuming polynomial (4), sigmoid (5) and cubic-splines (6), ϑ_n can be written as [11]:

$$\vartheta_n = \begin{cases} \left[\gamma_1, \gamma_2, ..., \gamma_m \right], & \text{polynomial case} \\ \left[\gamma_1, \gamma_2, \gamma_3 \right], & \text{sigmoid case} \\ \left[\gamma_1, \gamma_2, ..., \gamma_5 \right] & \text{spline case} \end{cases}. \tag{10}$$

The output of ESM models of cubic-spline, polynomial, and sigmoid functions are expressed, as:

$$x(t) = -\left(\sum_{i=1}^{n_q} q_i z^{-i} \right) x(t) + \left(\sum_{i=1}^{n_p} p_i z^{-i} \right) \sum_{i=1}^{m-2} \left(\begin{array}{l} \gamma_i \left| u(t) - u_{i+1}(t) \right|^3 + \gamma_{m-1} + \\ \gamma_m u(t) + \gamma_{m+1} u^2(t) + \gamma_{m+2} u^3(t) \end{array} \right) + n(t). \tag{11}$$

$$x(t) = -\left(\sum_{i=1}^{n_q} q_i z^{-i} \right) x(t) + \left(\sum_{i=1}^{n_p} p_i z^{-i} \right) \left(\gamma_1 . \frac{e^{\gamma_2 u(t)} - 1}{e^{\gamma_2 u(t)} + \gamma_3} \right) + n(t), \tag{12}$$

$$x(t)=-\left(\sum_{i=1}^{n_q}q_i z^{-i}\right)x(t)+\left(\sum_{i=1}^{n_p}p_i z^{-i}\right)\left(\gamma_1 u(t)+\gamma_2 u^2(t)+\cdots+\gamma_m u^m(t)\right)+n(t), \tag{13}$$

Corresponding output from ESM for cubic-spline, sigmoid and polynomial at k instances are written as:

$$x_k=-\left(\sum_{i=1}^{n_q}q_i z^{-i}\right)x_k+\left(\sum_{i=1}^{n_p}p_i z^{-i}\right)\sum_{i=1}^{m-2}\begin{pmatrix}\gamma_i\left|u_k-u_{k,i+1}\right|^3+\gamma_{m-1}+\\ \gamma_m u_k+\gamma_{m+1}u_k^2(t_k)+\gamma_{m+2}u_k^3\end{pmatrix}+n_k. \tag{14}$$

$$x_k=-\left(\sum_{i=1}^{n_q}q_i z^{-i}\right)x_k+\left(\sum_{i=1}^{n_p}p_i z^{-i}\right)\begin{pmatrix}\gamma_1 u_k+\gamma_2 u_k^2+\\ \cdots+\gamma_m u_k^m\end{pmatrix}+n_k, \tag{15}$$

$$x_k=-\left(\sum_{i=1}^{n_q}q_i z^{-i}\right)x_k+\left(\sum_{i=1}^{n_p}p_i z^{-i}\right)\begin{pmatrix}\gamma_1 u_k+\gamma_2 u_k^2+\\ \cdots+\gamma_m u_k^m\end{pmatrix}+n_k, \tag{16}$$

for $x_k=x(t_k)$, $u_k=u(t_k)$, $n_k=n(t_k)$ in case of k = 1, 2, …, K, where K is total number of instances.

Now task is to obtain the cost functions of ESM models by utilizing the formulation of mean square errors, ε as:

$$\varepsilon=\varepsilon_1+\varepsilon_2, \tag{17}$$

here, error function ε_1 is variation between the estimated $\boldsymbol{x}=[x_1,x_2,...,x_K]$ and the desired response $\hat{\boldsymbol{x}}=[\hat{x}_1,\hat{x}_2,...,\hat{x}_K]$, while and ε_2 is the mean square difference between estimated $\hat{\boldsymbol{\vartheta}}$ and desired $\boldsymbol{\vartheta}$ weight vectors. The mathematical expression for ε_1 is given as:

$$\varepsilon_1=\frac{1}{K}\sum_{k=1}^{K}\left(x_k-\hat{x}_k\right)^2, \tag{18}$$

Here, the k^{th} output of ESM model is x_k as in (14-16), while the $\hat{x}_k$ is the k^{th} output of estimated output response in terms of $\hat{\boldsymbol{\vartheta}}$ with polynomial $g(u)$:

$$\hat{\boldsymbol{\vartheta}}=\left[\hat{\boldsymbol{\vartheta}}_l,\hat{\boldsymbol{\vartheta}}_n\right]=\left[\hat{q}_1,\hat{q}_2,...,\hat{q}_{n_q},\hat{p}_1,\hat{p}_2,...,\hat{p}_{n_p},\hat{\gamma}_1,\hat{\gamma}_2,...,\hat{\gamma}_m\right], \tag{19}$$

$$\hat{x}_k=-\left(\sum_{i=1}^{n_q}q_i z^{-i}\right)\hat{x}_k+\left(\sum_{i=1}^{n_p}p_i z^{-i}\right)\begin{pmatrix}\gamma_1 u_k+\gamma_2 u_k^2+\\ \cdots+\gamma_m u_k^m\end{pmatrix},\qquad k=1,2,...,K \tag{20}$$

Accordingly, the estimated response $\hat{\boldsymbol{x}}$ with approximate parameter vector $\hat{\boldsymbol{\vartheta}}$ by taking sigmoid as basis function is written as:

$$\hat{\vartheta} = \left[\hat{\vartheta}_l,\ \hat{\vartheta}_n \right] = \left[\hat{q}_1, \hat{q}_2, ..., \hat{q}_{n_q}, \hat{p}_1, \hat{p}_2, ..., \hat{p}_{n_p}, \hat{\gamma}_1, \hat{\gamma}_2, ..., \hat{\gamma}_m \right], \tag{21}$$

$$\hat{x}_k = -\left(\sum_{i=1}^{n_q} q_i z^{-i} \right) \hat{x}_k + \left(\sum_{i=1}^{n_p} p_i z^{-i} \right) \left(\gamma_1 . \frac{e^{\gamma_2 u_k} - 1}{e^{\gamma_2 u_k} + \gamma_3} \right), \qquad k = 1, 2, ..., K \tag{22}$$

Similarly, the estimated response $\hat{\boldsymbol{x}}$ with $\hat{\vartheta}$ for cubic-spline $g(u)$ is described as:

$$\hat{\vartheta} = \left[\hat{\vartheta}_l,\ \hat{\vartheta}_n \right] = \left[\hat{q}_1, \hat{q}_2, ..., \hat{q}_{n_q}, \hat{p}_1, \hat{p}_2, ..., \hat{p}_{n_p}, \hat{\gamma}_1, \hat{\gamma}_2, ..., \hat{\gamma}_m \right], \tag{23}$$

$$\hat{\boldsymbol{x}}_k = -\left(\sum_{i=1}^{n_q} q_i z^{-i} \right) \hat{\boldsymbol{x}}_k + \left(\sum_{i=1}^{n_p} p_i z^{-i} \right) \sum_{i=1}^{m-2} \begin{pmatrix} \gamma_i \left| u_k - u_{k,i+1} \right|^3 + \gamma_{m-1} + \\ \gamma_m u_k + \gamma_{m+1} u_k^2 + \gamma_{m+2} u_k^3 \end{pmatrix}, \qquad k = 1, 2, ..., K \tag{24}$$

The error function ε_2 is mathematically described as a mean squared error between the estimated and desired ESM parameters:

$$\varepsilon_2 = \frac{1}{N} \sum_{k=1}^{N} \left(\vartheta_k - \hat{\vartheta}_k \right)^2. \tag{25}$$

Here, N represents the total number of elements in the parameter vector, ϑ_k and $\hat{\vartheta}_k$ denotes the k^{th} entity of desired and estimated weight vector, respectively. For input nonlinear functions $g(u)$, the parameter N is $n_q + n_p + m$ for polynomial, $n_q + n_p + 3$ for sigmoid, and $n_q + n_p + m$ for cubic-spline. So the objective function (17) using (18) and (25) is written as:

$$\varepsilon = \frac{1}{K} \sum_{k=1}^{K} \left(x_k - \hat{x}_k \right)^2 + \frac{1}{N} \sum_{k=1}^{N} \left(\vartheta_k - \hat{\vartheta}_k \right)^2, \tag{26}$$

Next step is to utilize the heuristic schemes to obtain the solution of the ESM models (26) by finding the optimal parameters of $\hat{\vartheta}$ so that $\varepsilon \to 0$, as error approaches zero, estimated solution approaches the desired solution, *i.e.*, $\hat{\boldsymbol{x}} \to \boldsymbol{x}$, therefore consequently, the estimated parameter vector approaches its optimal, i.e., $\hat{\vartheta} \to \vartheta$.

2.2 Optimization Mechanism for ESMs

A brief introduction of evolutionary computing optimization algorithms based on DE and GAs is presented here. These optimization solvers are exploited to obtain actual parameters by optimizing ESM model merit function (14). These algorithms may be exploited as a part of iterative learning control based hardware, if optimization of the decision variable is efficient and accurate then relatively lesser processing power as well as storage capacity is required that definitely assist to reduce the cost of the equipment's.

DE is the member of evolutionary search strategies developed by Storn and Price for continuous domains optimization problems [74-75]. DE is one of best population based technique having

benefits of simplicity, effortless implementation; speedy convergence and robustness for finding solution of real valued parameters. DE employs mutation as a search technique and selection is used to direct the prospective search toward the feasible region. DE has been broadly utilized to solve real world problems in engineering domain such as simultaneous transit network design [76], facial expression recognition systems [77], self-paced stacked denoising autoencoders [78], optimal reactive power dispatch systems [79], optimized watermarking [80] and image processing [81].

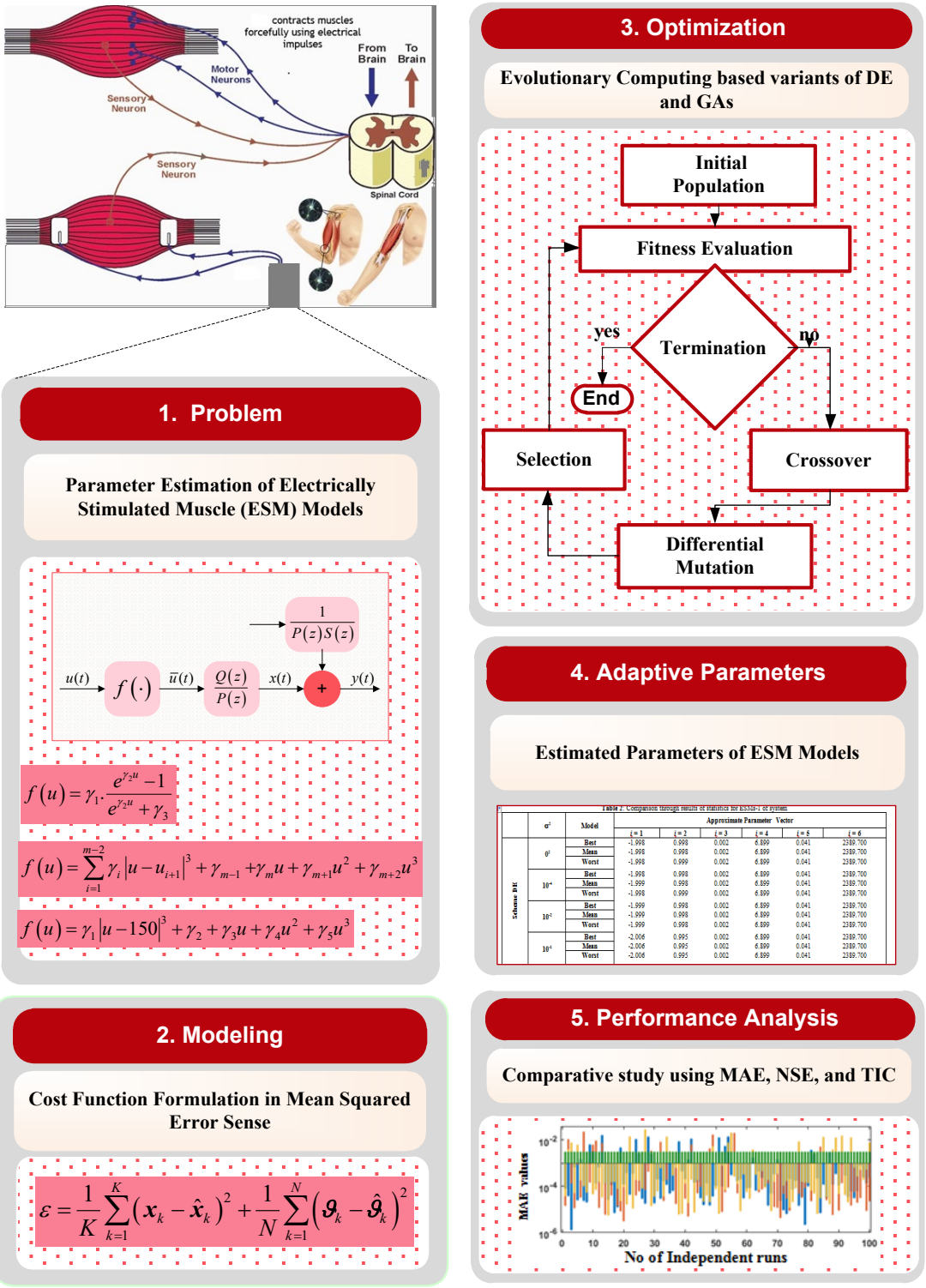

Fig. 1: Schematic diagram of proposed methodologies

Genetic algorithms is one of the best global search procedure belonging to the class of evolutionary computing heuristics. GAs are introduced by Holland [82-83], on the basis of simple mathematical modeling of genetics. Normally, GAs operate with three fundamental operators used in reproduction of the population at each generation based on selection, mutation and crossover. GAs

is widely employed for different optimization problems of engineering and applied sciences including sentiment analysis of microblogs [84], viable intrusion detection system design [85], disassembly sequence planning problems [86], transit network design problems [87], feature selection for credit rating problems [88] and optimization of Sisko fluid flow based heat transfer models [89].

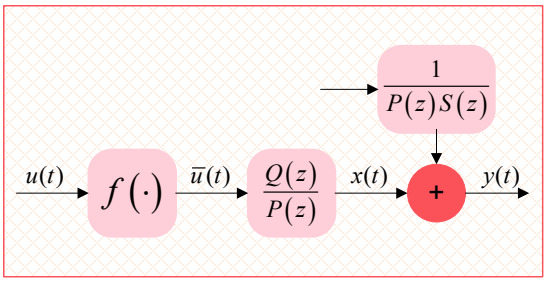

Fig. 2. The Hammerstein control autoregressive block structure

Effectiveness of these meta-heuristic algorithms based on DE and GAs motivates authors to exploit the strength of evolutionary optimization procedures in obtaining the optimization variables of ESM models. Besides that, the procedure of PSO, PS and SA with settings of the parameter as given in the references [90-92] are also implemented for finding the decision variables of ESM model. Generic flow diagram of DE is illustrated in Fig. 3 while stepwise procedure is described in Table. 1

Table 1: Pseudocode for DE algorithm for identification problem of ESM models

Part 1: DE

Input:

A chromosome or individual $\boldsymbol{C}$ by means of optimization variable is defined as:

$$\boldsymbol{C} = [\vartheta] = [\vartheta_1, \vartheta_2, ..., \vartheta_n]$$

Population of Chromosomes $\boldsymbol{C}$ **is given as:**

$$\boldsymbol{P_C} = \begin{bmatrix} \boldsymbol{C}_1 \\ \boldsymbol{C}_2 \\ \vdots \\ \boldsymbol{C}_d \end{bmatrix} = \begin{bmatrix} \vartheta_1 \\ \vartheta_2 \\ \vdots \\ \vartheta_d \end{bmatrix} = \begin{bmatrix} \vartheta_{1,1} & \vartheta_{1,2} & \cdots & \vartheta_{1,n} \\ \vartheta_{2,1} & \vartheta_{2,2} & \cdots & \vartheta_{2,n} \\ \vdots & \vdots & \vdots & \vdots \\ \vartheta_{d,1} & \vartheta_{d,2} & \cdots & \vartheta_{d,n} \end{bmatrix},$$

Output:

Returned the optimization variables of ESM with DE, $\mathbf{C_{DE}}$, $\boldsymbol{C}_{DE} = [\vartheta]_{best}$ with $\min \varepsilon$ as in equation(26).

Begin DE

```
//Initialization of parameters
crossover probability (CR)= 0.9,
scaling factor (F)= 0.5,
population size (P)= 60, i.e., d in C
dimensionality (D), i.e., n in C
//Randomly generate G
for k= 1 to P do
      For j= 1 to D do
```

$\vartheta_{j,k}^{(G=0)} = \vartheta_j^{min} + rand_j[0,1].(\vartheta_j^{max} - \vartheta_j^{min})$

end for

end for

//calculate ε

//For each *C* calculate ε as as defined for ESM model

for *k*= 1 to P **do**

$\varepsilon_{\vartheta}|_k^{G+1}$

end for

// Generate Test vectors using recombination operators

for *k*= 1 to Gen_{max} **do**

//Select three random vectors

for *l*= 1 to *P* **do**

select randomly $r_1, r_2, r_3 \in [1, P], r_1 \neq r_2 \neq r_3 \neq k$

//N each ϑ undergoes mutation, crossover operation

//Generate random integer $jrand \in [1, P]$

for *j* = 1 to D **do**

if*(rand[0,1]<CR or j==jrand)* **then**

$v_{j,k}^{(G+l)} = \vartheta_{k,r1}^{(G)} + F * (\vartheta_{k,r2}^{(G)} - \vartheta_{k,r3}^{(G)})$

Else

$v_{j,k}^{(G+l)} = \vartheta_{k,\mathrm{j}}^{(G)}$

end if

end for

end for

//Selection Step

if $\left(\varepsilon_{v}|_k^{G+1} \leq \varepsilon_{\vartheta}|_k^{G+1}\right)$ **then**

$\vartheta_k^{(G+1)} = v_{k,j}^{(G+l)}$

Else

$\vartheta_k^{(G+1)} = \vartheta_k^{(G)}$

endif

end for

End DE

//Accumulation step

Store C_{best} with its ε, elapsed time, generation consumed for the current run of the DE.

End Part 1

Part 2: Statistics

In order to get appropriate parameter of ESM model repeat the procedure for several independent runs to generate a dataset for effective performance analysis of proposed scheme.

End Part 2

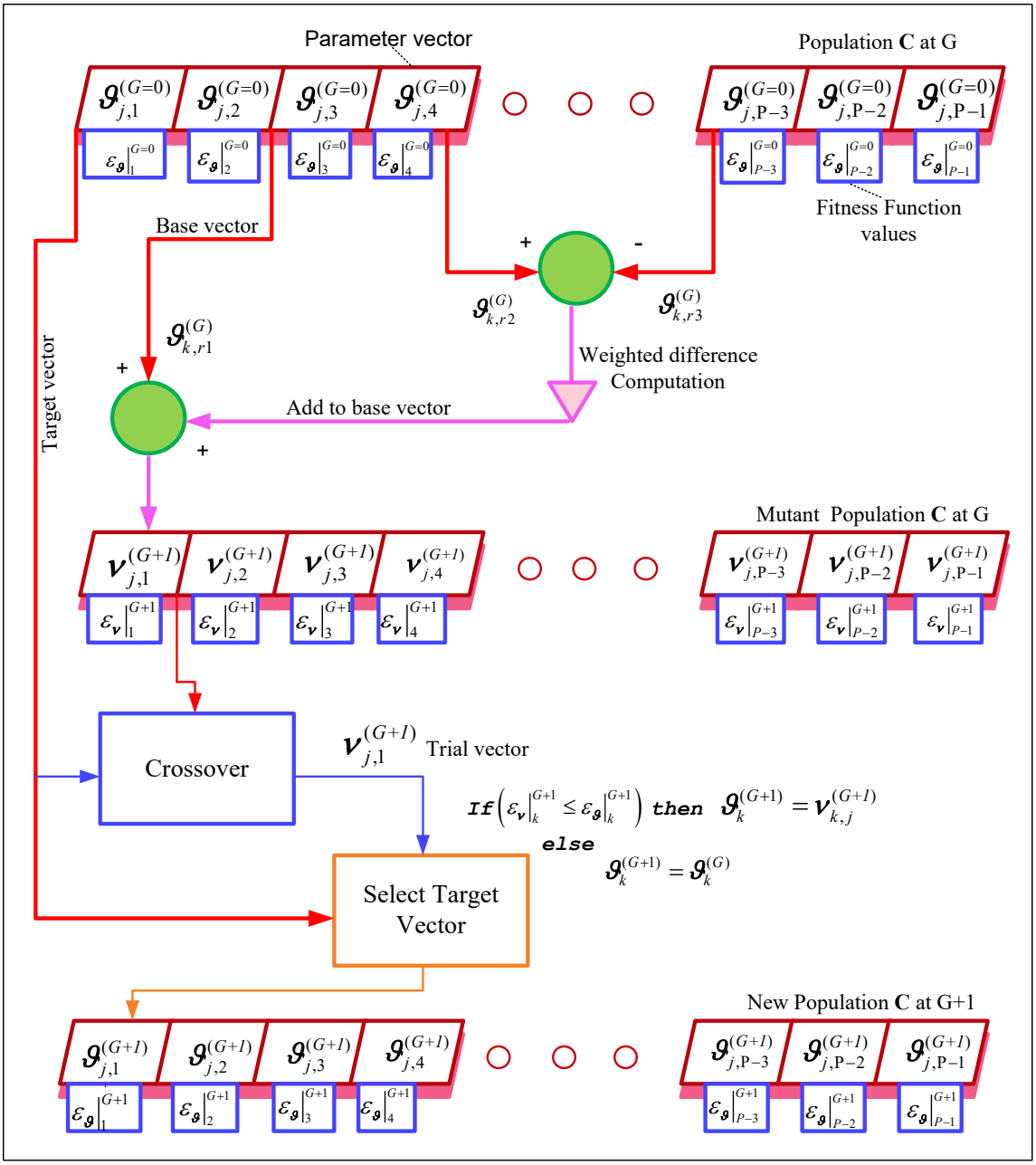

Fig. 3: Workflow diagram of DE for ESM model estimation of parameters

3 Performance Operators

The performance indices for ϑ in terms of mean absolute error (MAE_{ϑ}), normalizing error function, δ_{ϑ}, Thiel's inequality coefficient, (TIC_{ϑ}) and Nash Sutcliffe efficiency (NSE_{ϑ}) are utilized to access the designed schemes for parameter estimation of ESM models. The mathematical relations of all these operators are written as follows.

The MAE_{ϑ} is defined as:

$$MAE_{\vartheta} = \frac{1}{n}\sum_{i=1}^{n}\left|\vartheta_i - \hat{\vartheta}_i\right|, \tag{27}$$

here ϑ_i is the i^{th} element of actual parameter vector ϑ_i.

Thiel's Inequality Coefficient (TIC_{ϑ}) is mathematically written as:

$$TIC_{\vartheta} = \frac{\sqrt{\frac{1}{n}\sum_{i=1}^{n}\left(\vartheta_i - \hat{\vartheta}_i\right)^2}}{\left(\sqrt{\frac{1}{n}\sum_{i=1}^{n}\vartheta_i^2} + \sqrt{\frac{1}{n}\sum_{i=1}^{n}\hat{\vartheta}_i^2}\right)}, \tag{28}$$

Normalize error function (NEF) in term of mean weigh deviation

$$\delta_{\vartheta} = \frac{\left\|\hat{\vartheta} - \vartheta\right\|}{\left\|\vartheta\right\|}, \tag{29}$$

where $\|\ \|$ is the standard L^2 norm.

Nash Sutcliffe efficiency (NSE_{ϑ}) is formulated as:

$$NSE_{\vartheta} = 1 - \frac{\sum_{i=1}^{n}(\vartheta_i - \hat{\vartheta}_i)^2}{\sum_{i=1}^{n}(\vartheta_i - \overline{\vartheta}_i)^2}, \tag{30}$$

and its related error term $ENSE_{\vartheta}$ is $1 - NSE_{\vartheta}$.

Similarly, the global version of MAE_{ϑ} ($GMAE_{\vartheta}$) is formalized as:

$$GMAE_{\vartheta} = \frac{1}{I_E}\sum_{e=1}^{I_E}\left(MAE_{\vartheta}\right)_e = \frac{1}{I_E}\sum_{e=1}^{I_E}\left(\frac{1}{n}\sum_{i=1}^{n}\left|\vartheta_i - \hat{\vartheta}_i\right|\right)_e, \tag{31}$$

here, symbol I_E denotes the total number of independent executions.

Global TIC_{ϑ} ($G_{TIC\vartheta}$) is formulated as:

$$G_{TIC\vartheta} = \frac{1}{I_E}\sum_{e=1}^{I_E}\left(TIC_{\vartheta}\right)_e = \frac{1}{I_E}\sum_{e=1}^{I_E}\left(\frac{\sqrt{\frac{1}{n}\sum_{i=1}^{n}\left(\vartheta_i - \hat{\vartheta}_i\right)^2}}{\left(\sqrt{\frac{1}{n}\sum_{i=1}^{n}\vartheta_i^2} + \sqrt{\frac{1}{n}\sum_{i=1}^{n}\hat{\vartheta}_i^2}\right)}\right)_e. \tag{32}$$

Accordingly, global version of Nash Sutcliffe efficiency (NSE_{ϑ}) is formulated as:

$$G_{NSE\vartheta} = \frac{1}{I_E}\sum_{e=1}^{I_E}\left(NSE_{\vartheta}\right)_e = \frac{1}{I_E}\sum_{e=1}^{I_E}\left(1-\frac{\sum_{i=1}^{n}(\vartheta_i-\hat{\vartheta}_i)^2}{\sum_{i=1}^{n}(\vartheta_i-\bar{\vartheta}_i)^2}\right)_e. \tag{33}$$

Additionally, mean fitness $\bar{\varepsilon}_{\vartheta}$ in terms of total number of executions I_E is formulated as:

$$\bar{\varepsilon}_{\vartheta} = \frac{1}{I_E}\sum_{e=1}^{I_E}\left(\varepsilon_{\vartheta}\right)_e = \frac{1}{I_E}\sum_{e=1}^{I_E}\left(\frac{1}{K}\sum_{k=1}^{K}\left(x_k-\hat{x}_k\right)^2+\frac{1}{N}\sum_{k=1}^{N}\left(\vartheta_k-\hat{\vartheta}_k\right)^2\right)_e \tag{34}$$

In the ideal case, values of the performance indices must be zero.

4. Experimentation and Results

Results for parameter estimation for three ESM models are presented through DE and GAs based evolutionary computational heuristics. In all three ESM systems, the performance of both optimization solvers is evaluated and presented here for a noiseless scenario as well as three noisy cases with different variances, *i.e.*, $\sigma^2 = 0.001^2, 0.01^2$, and 0.1^2.

ESM-I: *ESM model with sigmoid Kernel based input nonlinearity*: The parameters estimation of ESM-1 based on available dataset reported in [11] as followings:

$$\begin{aligned}
&x(t) = \frac{P(z)}{Q(z)}g\left(u(t)\right)+\frac{1}{Q(z)}n(t),\\
&Q(z) = 1+q_1z^{-1}+q_2z^{-2} = 1-1.9985z^{-1}+0.9985z^{-2},\\
&P(z) = p_1z^{-1} = 0.0022z^{-1},\\
&f\left(u(t)\right) = \gamma_1.\frac{e^{\gamma_2u(t)}-1}{e^{\gamma_2u(t)}+\gamma_3} = 6.8994.\frac{e^{0.0410u(t)}-1}{e^{0.0410u(t)}+2389.70},\\
&x(t) = -\left[-1.9985x\left(t-1\right)+0.9985x\left(t-2\right)\right]\\
&\qquad +0.0022\left[6.8994\times\frac{e^{0.0410u(t-1)}-1}{e^{0.0410u(t-1)}+2389.7}\right]+n\left(t\right),\\
&\vartheta = \left[q_1,q_2,p_1,\gamma_1,\gamma_2,\gamma_3\right],\\
&\vartheta = \left[-1.9985,0.9985,0.0022,6.8994,0.0410,2389.70\right].
\end{aligned} \tag{35}$$

The fitness evaluation function for ESM-I is constructed accordingly to equation (26) by taking $K = 20$ and $N = 6$ as:

$$\varepsilon = \frac{1}{20}\sum_{k=1}^{20}\left(x_k-\hat{x}_k\right)^2+\frac{1}{6}\sum_{k=1}^{6}\left(\vartheta_k-\hat{\vartheta}_k\right)^2 \tag{36}$$

ESM-II: *ESM model with polynomial* $g(u(t))$**:** The parameters estimation of ESM-II system *with* polynomial kernel $g(u(t))$ based on available dataset reported in [11] as followings:

$$
\begin{aligned}
&x(t)=\frac{P(z)}{Q(z)}g(u(t))+\frac{1}{Q(z)}n(t),\\
&Q(z)=1+q_1z^{-1}+q_2z^{-2}=1-z^{-1}+0.8z^{-2},\\
&P(z)=p_1z^{-1}+p_2z^{-2}=z^{-1}+0.6z^{-2},\\
&f(u(t))=\gamma_1u(t)+\gamma_2u^2(t)+\gamma_3u^3(t)=2.8u(t)-4.8u^2(t)+5.7u^3(t),\\
&x(t)=-\left[-1.00x(t-1)+0.8x(t-2)\right]+\left[(1)(2.8)\right]u(t-1)\\
&\qquad+\left[(1)(-4.8)\right]u^2(t-1)+\left[(1)(5.7)\right]u^3(t-1)+\left[(0.6)(2.8)\right]u(t-2)\\
&\qquad+\left[(0.6)(-4.8)\right]u^2(t-2)+\left[(0.6)(5.7)\right]u^3(t-2)+n(t),\\
&\vartheta=\left[q_1,q_2,p_1,p_2,\gamma_1,\gamma_2,\gamma_3\right],\\
&\vartheta=\left[-1.00,0.80,1.00,0.60,2.80,-4.80,5.70\right].
\end{aligned}
\tag{37}
$$

The fitness function constructed on similar pattern used for ESM-I and given for the said case as:

$$
\varepsilon=\frac{1}{20}\sum_{k=1}^{20}\left(x(t_k)-\hat{x}(t_k)\right)^2+\frac{1}{7}\sum_{k=1}^{7}\left(\vartheta_k-\hat{\vartheta}_k\right)^2. \tag{38}
$$

ESM-III: *ESM model with cubic-spline* $g(u(t))$: The parameters estimation of EMS-II model *with* cubic-spline kernel $g(u(t))$ have one know at 150 based on available dataset reported in [11] as followings:

$$
\begin{aligned}
&x(t)=\frac{P(z)}{Q(z)}g(u(t))+\frac{1}{Q(z)}n(t),\\
&Q(z)=1+q_1z^{-1}+q_2z^{-2}=1-1.094z^{-1}+0.109z^{-2},\\
&P(z)=p_1z^{-1}+p_2z^{-2}=z^{-1}+0.249z^{-2},\\
&f(u(t))=\gamma_1+\gamma_2u(t)+\gamma_3u^2(t)+\gamma_4u^3(t)+\gamma_5\left|u^3(t)-150\right|,\\
&f(u(t))=-0.028+1.90\times10^{-3}u(t)-7.83\times10^{-6}u^2(t)\\
&\qquad+1.78\times10^{-8}u^3(t)+2.36\times10^{-8}\left|u^3(t)-150\right|,
\end{aligned}
\tag{39}
$$

$$
\begin{aligned}
x(t) = &-\left[-1.094x(t-1)+0.109x(t-2)\right]+\left[(1)(-0.028)\right] \\
&+\left[(1)\left(1.90\times10^{-3}\right)\right]u(t-1)+\left[(1)\left(-7.83\times10^{-6}\right)\right]u^2(t-1) \\
&+\left[(1)\left(1.78\times10^{-8}\right)\right]u^3(t-1)+\left[(1)\left(2.36\times10^{-8}\right)\right]\left|u^3(t-1)-150\right| \\
&+\left[(0.249)(-0.028)\right]+\left[(0.249)\left(1.90\times10^{-3}\right)\right]u(t-1) \\
&+\left[(0.249)\left(-7.83\times10^{-6}\right)\right]u^2(t-1)+\left[(0.249)\left(1.78\times10^{-8}\right)\right]u^3(t-1) \\
&+\left[(0.249)\left(2.36\times10^{-8}\right)\right]\left|u^3(t-1)-150\right|+n(t),
\end{aligned}
$$

$$
\vartheta = \left[q_1, q_2, p_1, p_2, \gamma_1, \gamma_2, \gamma_3, \gamma_4, \gamma_5\right],
$$

$$
\vartheta = \begin{bmatrix} -1.094, 0.109, 1.00, -0.249, -0.028, \\ 1.90\times10^{-3}, -7.83\times10^{-6}, 1.78\times10^{-8}, 2.36\times10^{-8} \end{bmatrix}.
$$

The fitness function for ESM-III is formulated for K = 20 and N = 9 as:

$$
\varepsilon = \frac{1}{20}\sum_{k=1}^{20}\left(x(t_k)-\hat{x}(t_k)\right)^2+\frac{1}{9}\sum_{k=1}^{9}\left(\vartheta_k-\hat{\vartheta}_k\right)^2 \tag{40}
$$

The designed heuristic techniques based on DE and GAs have been performed for 100 independent trails to optimize the fitness functions for all three ESM models in case of noiseless and noisy scenarios. The results of DE and GAs on the basis of learning curves, i.e., iterative convergence plots, are presented in the graphical form in Fig. 4, for both ESM-I and ESM-II, in case of four noise variances σ^2 = 0.001^2, 0.01^2, 0.1^2 and 0. In all these plots, it is observed that for each noise scenario both DE and GAs are convergent, but DE attains better fitness.

To access the level of the accuracy attained by the algorithms, magnitudes of absolute error (AE) are computed for each case of all three ESM models for noise levels σ^2 = 0.001^2, 0.01^2, 0.1^2 and 0. The results are presented in Figs. 5-6 for the best trials of DE and GAs based on minimum fitness, respectively. The magnitudes of AE are found close to 10^{-09} to 10^{-12}, 10^{-09} to 10^{-12}, 10^{-09} to 10^{-11} and 10^{-04} to 10^{-11} for noise variances σ^2 = 0.001^2, 0.01^2, 0.1^2 and 0, respectively, for DE, while for GAs respective AE are found close to 10^{-08} to 10^{-09}, 10^{-04} to 10^{-08}, 10^{-05} to 10^{-11} and 10^{-04} to 10^{-7}. It is also noticed that the designed scheme is convergent for all three ESM systems, but a small degradation in the accuracy of the techniques is observed with an increase in the nose levels, for both algorithms.

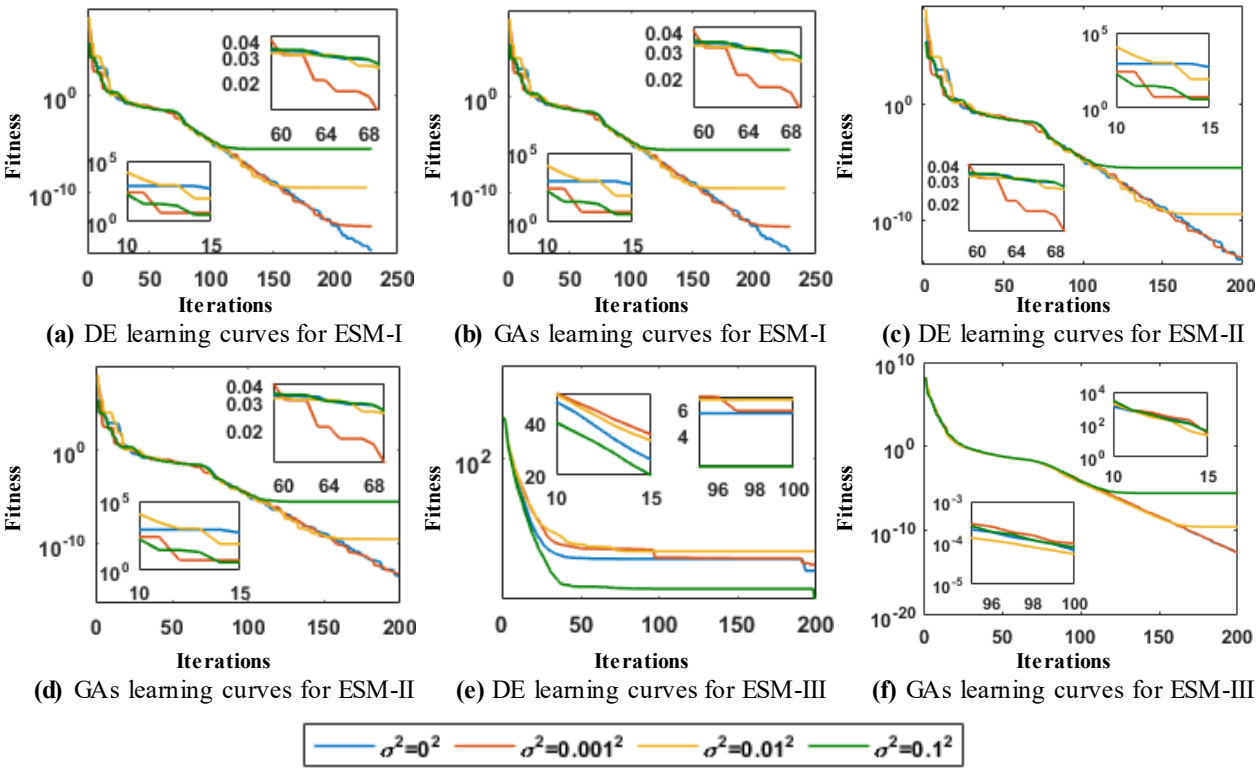

(a) DE learning curves for ESM-I **(b)** GAs learning curves for ESM-I **(c)** DE learning curves for ESM-II

(d) GAs learning curves for ESM-II **(e)** DE learning curves for ESM-III **(f)** GAs learning curves for ESM-III

Fig. 4. Results for convergence analysis of merit function of ESM-I, II and III

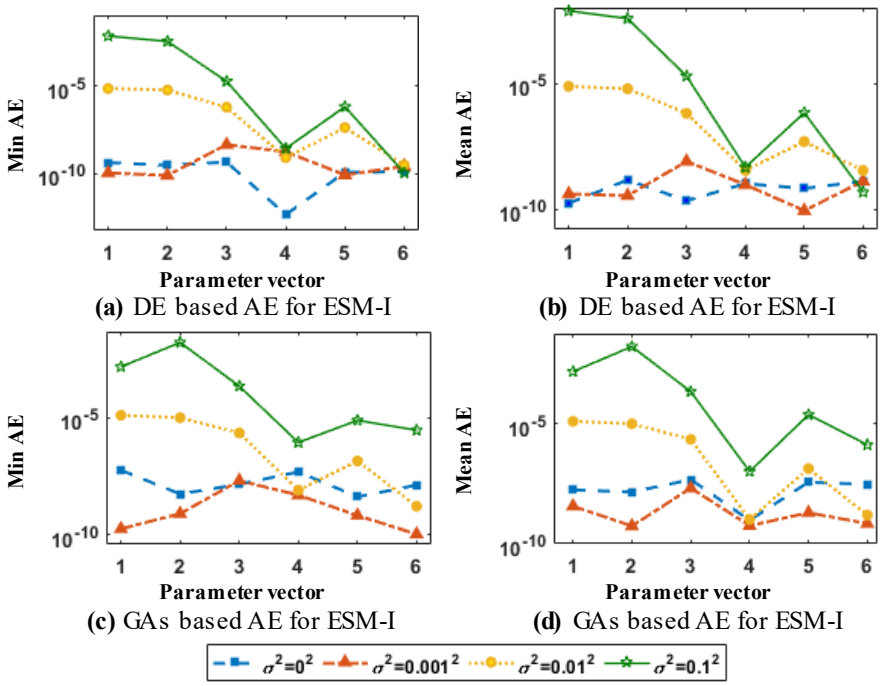

(a) DE based AE for ESM-I **(b)** DE based AE for ESM-I

(c) GAs based AE for ESM-I **(d)** GAs based AE for ESM-I

Fig. 5. Comparison of absolute error for ESM-1 systems with different noise levels

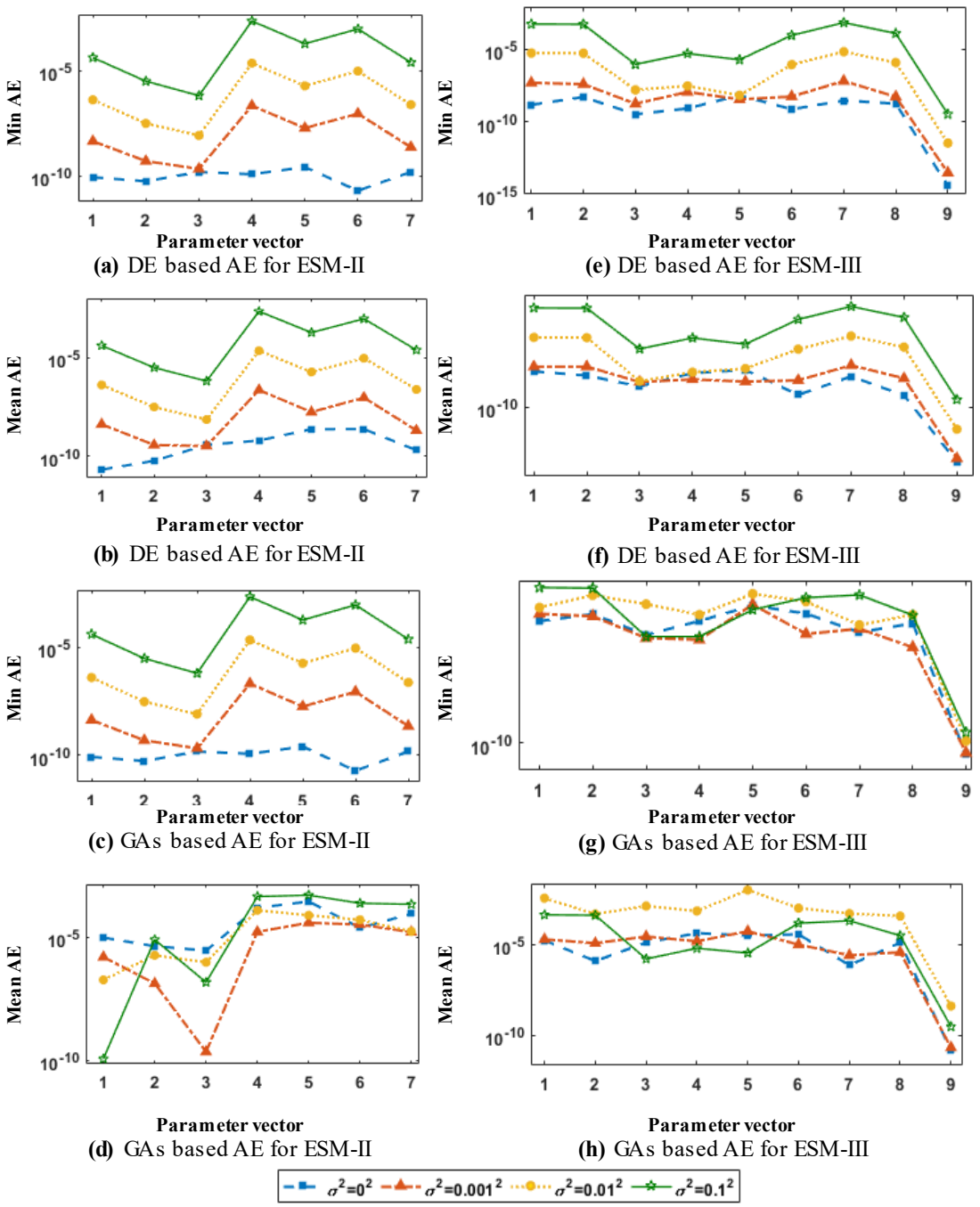

Fig. 6. Comparison on AE for ESM-II and III systems with different noise levels

The evaluation of for both DE and GAs is performed through performance indices based on accuracy criterion of fitness ε, normalized error function δ_g, MAE_g, NSE_g, and TIC_g, as described mathematically in the last section. Results on the basis of best fitness are presented in Table 2 along with the complexity operators in terms of time, cycles and function counts. It can be seen that the MWD, δ lie around 10^{-03} to 10^{-08}, 10^{-03} to 10^{-08} in case of ESM-I for both DE and GAs, respectively, while for ESM-II values are found close to 10^{-03}, whereas in case of ESM-III respective values of DE and GAs ranges between 10^{-03} to 10^{-05}, and 10^{-03} to 10^{-09}. In general, the

significantly near-optimal gauges of these performance operators are obtained which ascertains the consistent accuracy of the proposed schemes, however DE is placed at the higher ranks by achieving relatively lower values of the indices than that of GAs.

Table 2: Comparison of the performance on basis of best runs of both algorithms for each variant of ESM models

Solver	ESM	σ^2	Accuracy					Complexity		
			ε	δ	MAE	NSE	TIC	Time	Gens	FC
DE	I	**0**	8.86E-20	3.05E-13	2.43E-10	0.00E+00	4.92E-13	7.81	192	34751
		10^{-3}	3.34E-12	6.83E-13	1.16E-09	0.00E+00	1.72E-12	7.64	217	39276
		10^{-2}	3.34E-08	5.67E-13	2.40E-06	0.00E+00	2.05E-09	7.47	208	37647
		10^{-1}	1.83E-04	1.66E-12	1.87E-03	7.33E-11	1.75E-06	7.79	215	38914
	II	**0**	4.56E-18	1.64E-12	1.20E-10	0.00E+00	2.05E-10	10.69	191	40300
		10^{-3}	9.61E-14	7.19E-13	4.63E-08	3.79E-14	1.41E-08	9.69	176	37135
		10^{-2}	9.60E-10	1.79E-12	4.83E-06	4.15E-10	1.47E-06	9.77	181	38190
		10^{-1}	9.60E-06	2.01E-12	1.87E-03	4.15E-06	1.47E-04	9.64	179	37768
	III	**0**	1.26E-16	6.23E-13	2.14E-09	2.22E-16	2.93E-09	19.12	236	63955
		10^{-3}	3.14E-14	7.97E-13	1.94E-08	2.69E-14	2.82E-08	17.00	220	59619
		10^{-2}	3.12E-10	1.15E-12	2.12E-06	3.73E-10	3.32E-06	16.78	220	59619
		10^{-1}	3.12E-06	3.59E-13	1.87E-03	3.69E-06	3.29E-04	24.96	230	62329
GAs	I	**0**	9.87E-16	3.22E-11	2.36E-08	0.00E+00	1.48E-11	10.37	300	60200
		10^{-3}	7.57E-12	3.21E-11	4.48E-09	0.00E+00	4.48E-12	11.16	300	60200
		10^{-2}	7.56E-08	3.04E-11	4.19E-06	2.22E-16	3.42E-09	9.72	300	60200
		10^{-1}	4.01E-04	2.66E-11	3.04E-03	2.87E-10	3.46E-06	10.64	300	60200
	II	**0**	8.90E-07	2.92E-11	1.18E-04	1.42E-07	2.00E-05	24.68	700	140200
		10^{-4}	1.24E-05	3.19E-11	2.41E-03	6.09E-05	5.63E-04	25.24	700	140200
		10^{-2}	1.90E-06	2.77E-11	1.90E-04	8.03E-08	2.05E-05	24.88	700	140200
		10^{-1}	1.30E-05	2.88E-11	3.04E-03	9.75E-07	7.13E-05	23.96	700	140200
	III	**0**	1.18E-09	3.13E-11	2.05E-05	2.13E-08	2.50E-05	20.64	500	100200
		10^{-4}	1.22E-09	2.61E-11	1.67E-05	2.82E-09	9.11E-06	21.33	500	100200
		10^{-2}	1.74E-08	3.21E-11	8.02E-05	2.13E-09	7.92E-06	19.99	500	100200
		10^{-1}	2.47E-06	3.23E-11	3.04E-03	1.36E-06	2.00E-04	21.01	500	100200

The reliability of the proposed scheme is examined through 100 independent runs in each noise scenario for all three examples of ESM models. The results in term fitness are presented in Fig. 7, while comparative analysis on the basis of performance indicators, i.e., MAE_g, NSE_g and TIC_g, are shown graphically in Figs. 8-9 for ESM-I, II and III, respectively. The TIC_g *graphs* for ESM-I for noise scenario $\sigma^2 = 0.001^2$ and $\sigma^2 = 0.01^2$ are illustrated graphically in Fig. 10, in the form of empirical cumulative distribution function plots for both DE and GAs. Additionally, the *MAE* for ESM-I and II are presented using semi-logarithmic scale in order to interpret small variation and are given in subfigures 11 (*a-b*) for DE and subfigures 11 (*c-d*) for GAs. These results show that the magnitudes of MAE for ESM-I are in the range of 10^{-04} to 10^{-20}, and 10^{-04} to 10^{-16} in case of DE and GAs, respectively. While for ESM-II values lie are in the range of 10^{-06} to 10^{-18}, and 10^{-05} to 10^{-07} for DE and GAs, respectively. Further accuracy evaluation of the proposed strategies is conducted through the plots of histogram and results on the basis of NSEs for ESM-I and II are presented in subfigures 11 (*e-h*) and subfigures. 11 (i-*l*) respectively. Furthermore, analysis on the basis of TIC for the two problems are presnted as stack bar plots in subfigures 11 (*m-n*) for DE and GAs, respectively. Moreover, ESM-III illustrations are provided in Fig. 12. All these graphs

validate the consistency of both the schemes designed for the parameter estimation problem of ESM systems for all four noise scenarios; Additional graph of comparison of both the studies is also provided in the form of bar plots and results are provided in Fig. 12 these results verify that DE outperforms GAs.

The detailed evaluation of the accuracy of the algorithm is carried out by statistical performance measures of mean, best, and worst magnitudes of fitness for $\sigma^2 = 0.001^2, 0.01^2$, and 0.1^2 as given in Table 3 for ESM-I along with the desired parameters. Similarly, the results for ESM-II and ESM-III are provided in Tables 4 and 5, respectively. It is observed that with the increase in noise level $\sigma^2 = 0.001^2$ to 0.1^2 degradation in the performance is noticed in case of both DE and GAs, however, both the algorithms are significantly applicable for finding the optimal ESM parameters with reasonable accuracy.

Table 3: Results of statistical operators for variants of ESM-I system

Solver	σ^2	Model	Approximate Parameter Vector					
			$i=1$	$i=2$	$i=3$	$i=4$	$i=5$	$i=6$
DE	0^2	Best	-1.998	0.998	0.002	6.899	0.041	2389.700
		Mean	-1.998	0.998	0.002	6.899	0.041	2389.700
		Worst	-1.998	0.999	0.002	6.899	0.041	2389.700
	10^{-4}	Best	-1.998	0.998	0.002	6.899	0.041	2389.700
		Mean	-1.999	0.998	0.002	6.899	0.041	2389.700
		Worst	-1.998	0.999	0.002	6.899	0.041	2389.700
	10^{-2}	Best	-1.999	0.998	0.002	6.899	0.041	2389.700
		Mean	-1.999	0.998	0.002	6.899	0.041	2389.700
		Worst	-1.999	0.998	0.002	6.899	0.041	2389.700
	10^{-1}	Best	-2.006	0.995	0.002	6.899	0.041	2389.700
		Mean	-2.006	0.995	0.002	6.899	0.041	2389.700
		Worst	-2.006	0.995	0.002	6.899	0.041	2389.700
GAs	0^2	Best	-1.998	0.999	0.002	6.899	0.041	2389.700
		Mean	-1.998	0.999	0.002	6.899	0.041	2389.700
		Worst	-1.998	0.998	0.002	6.899	0.041	2389.700
	10^{-4}	Best	-1.998	0.999	0.002	6.899	0.041	2389.700
		Mean	-1.998	0.999	0.002	6.899	0.041	2389.700
		Worst	-1.998	0.998	0.002	6.899	0.041	2389.700
	10^{-2}	Best	-1.999	0.998	0.002	6.899	0.041	2389.700
		Mean	-1.999	0.998	0.002	6.899	0.041	2389.700
		Worst	-1.999	0.998	0.002	6.899	0.041	2389.700
	10^{-1}	Best	-2.000	0.982	0.002	6.899	0.041	2389.700
		Mean	-2.000	0.982	0.002	6.899	0.041	2389.700
		Worst	-2.000	0.982	0.002	6.899	0.041	2389.700
True Parameter Vector			-1.998	0.998	0.002	6.899	0.041	2389.700

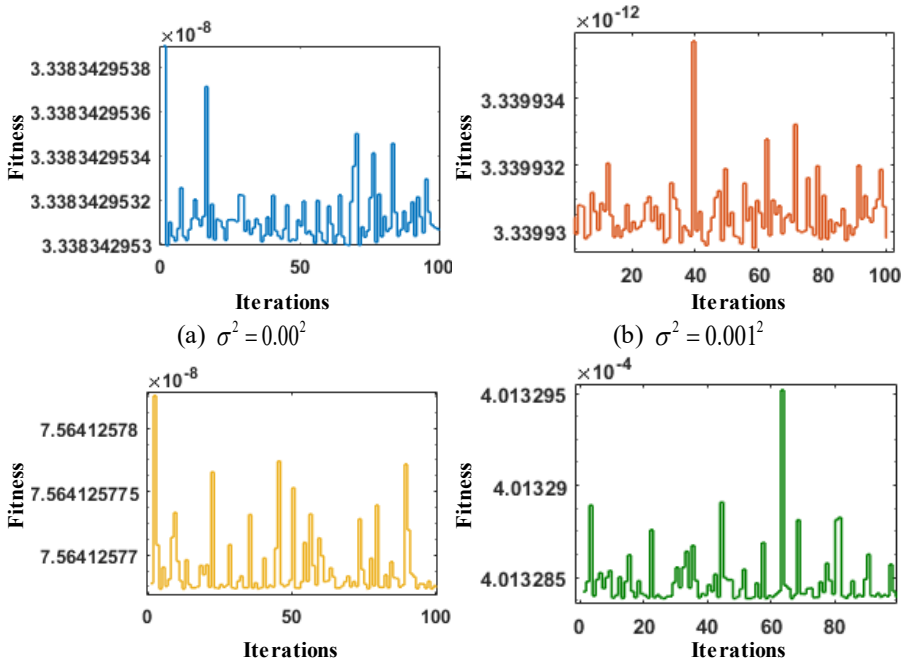

(a) $\sigma^2 = 0.00^2$ (b) $\sigma^2 = 0.001^2$

(c) $\sigma^2 = 0.01^2$ (d) $\sigma^2 = 0.1^2$

Fig. 7 Fitness plots for ESM-1 system with different noise levels using DE

Table 4: Results of statistical operators for variants of ESM-II system

Solver	Noise	Model	Approximate Parameter Vector						
			$i=1$	$i=2$	$i=3$	$i=4$	$i=5$	$i=6$	$i=7$
DE	0.000^2	Best	-1.000	0.800	1.000	2.800	-4.800	5.700	0.600
		Mean	-1.001	0.847	1.007	2.529	-4.434	5.364	0.432
		Worst	-1.016	1.511	2.276	-2.633	1.745	2.101	-3.618
	0.001^2	Best	-1.000	0.800	1.000	2.800	-4.800	5.700	0.600
		Mean	-0.996	0.858	0.857	2.561	-4.422	5.176	0.518
		Worst	-0.994	0.802	-3.561	-0.824	1.318	-1.543	-2.164
	0.010^2	Best	-1.000	0.800	1.000	2.800	-4.800	5.700	0.600
		Mean	-1.001	0.855	0.883	2.366	-4.185	5.110	0.307
		Worst	-0.994	0.802	-3.561	-0.824	1.318	-1.543	-2.164
	0.100^2	Best	-1.000	0.800	1.000	2.802	-4.800	5.699	0.600
		Mean	-1.000	0.819	0.956	2.749	-4.695	5.507	0.601
		Worst	-1.000	0.800	1.000	2.802	-4.800	5.699	0.00
GAs	0.000^2	Best	-1.000	0.800	1.000	2.800	-4.800	5.700	0.600
		Mean	-1.000	0.800	0.999	2.802	-4.803	5.703	0.600
		Worst	-1.000	0.800	1.000	2.800	-4.800	5.700	0.600
	0.001^2	Best	-1.000	0.800	0.999	2.803	-4.805	5.707	0.599
		Mean	-1.000	0.800	0.999	2.802	-4.803	5.703	0.600
		Worst	-1.000	0.800	1.000	2.800	-4.800	5.700	0.600
	0.010^2	Best	-1.000	0.800	1.000	2.800	-4.799	5.700	0.600
		Mean	-1.000	0.800	0.999	2.802	-4.804	5.705	0.600
		Worst	-1.000	0.800	1.000	2.800	-4.800	5.700	0.600
	0.100^2	Best	-1.000	0.800	1.000	2.799	-4.799	5.700	0.600
		Mean	-1.000	0.800	0.999	2.802	-4.803	5.705	0.600
		Worst	-1.000	0.800	1.000	2.799	-4.799	5.700	0.600
True Values			-1.000	0.800	1.000	2.800	-4.800	5.700	0.600

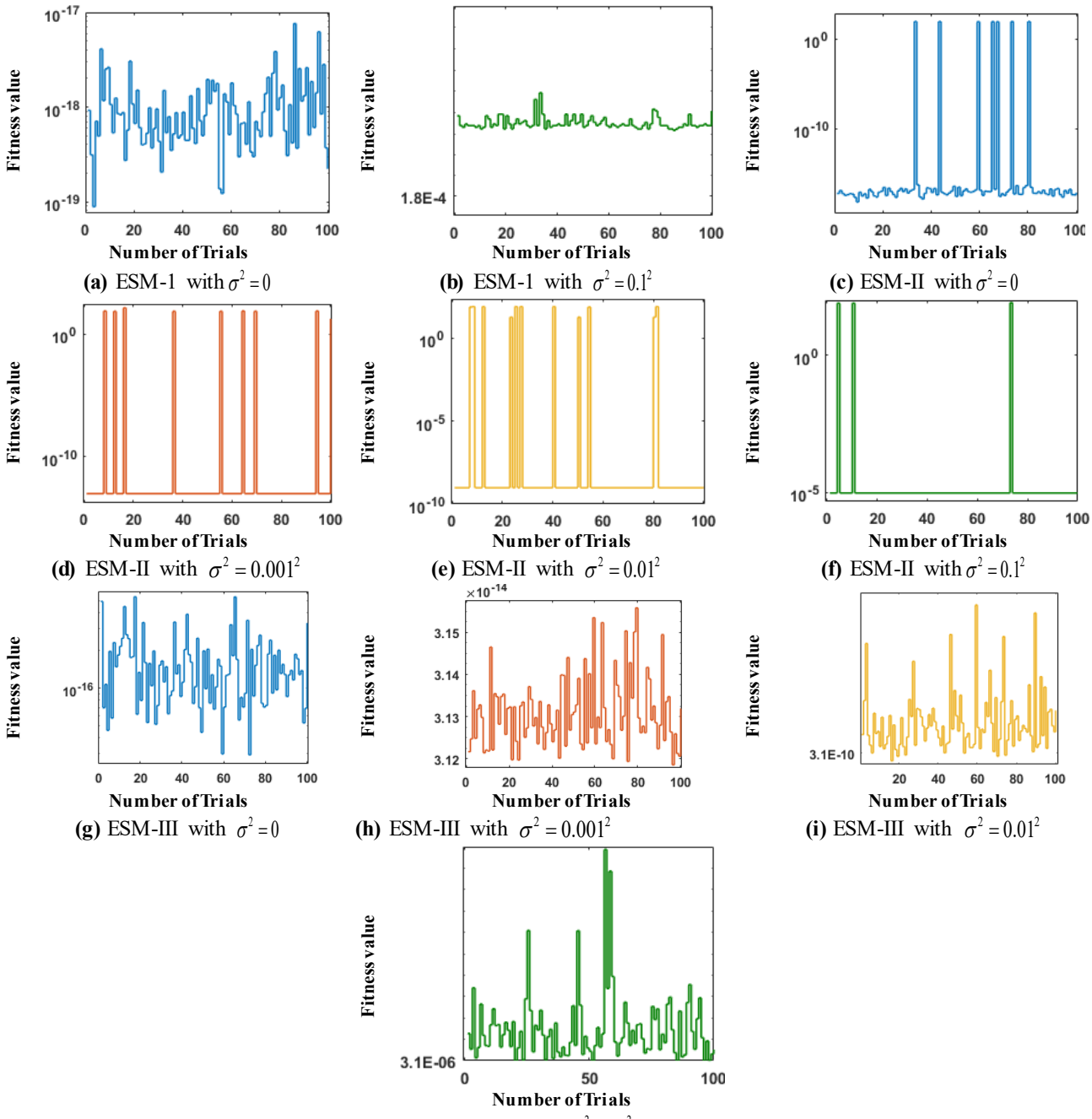

Fig. 8 Fitness plots for variants of ESM systems using GAs

Accuracy and convergence of both DE and GAs are analyzed through global evaluation metrics given in equations (30) - (33), with $I_e = 100$ and results are presented in Table 6 for all three ESM systems for all four noise variances. Generally, the magnitude of accuracy for global metrics based on mean fitness lie close to 10^{-04} to 10^{-18} in case of ESM-I, 10^{-05} to 10^{-17} for ESM-II, and 10^{-06} to 10^{-16} in case of ESM-III, for both DE and GAs, while similar trends for performance indices based on $GMAE_g$, $GNSE_g$, and $GTIC_g$ is observed for all the designed schemes. Very small magnitudes

of the global operators are generally acquired for all variants which verify the worth of the designed schemes for providing accurate, consistent, and convergent solutions for parameter estimation problem of ESM systems.

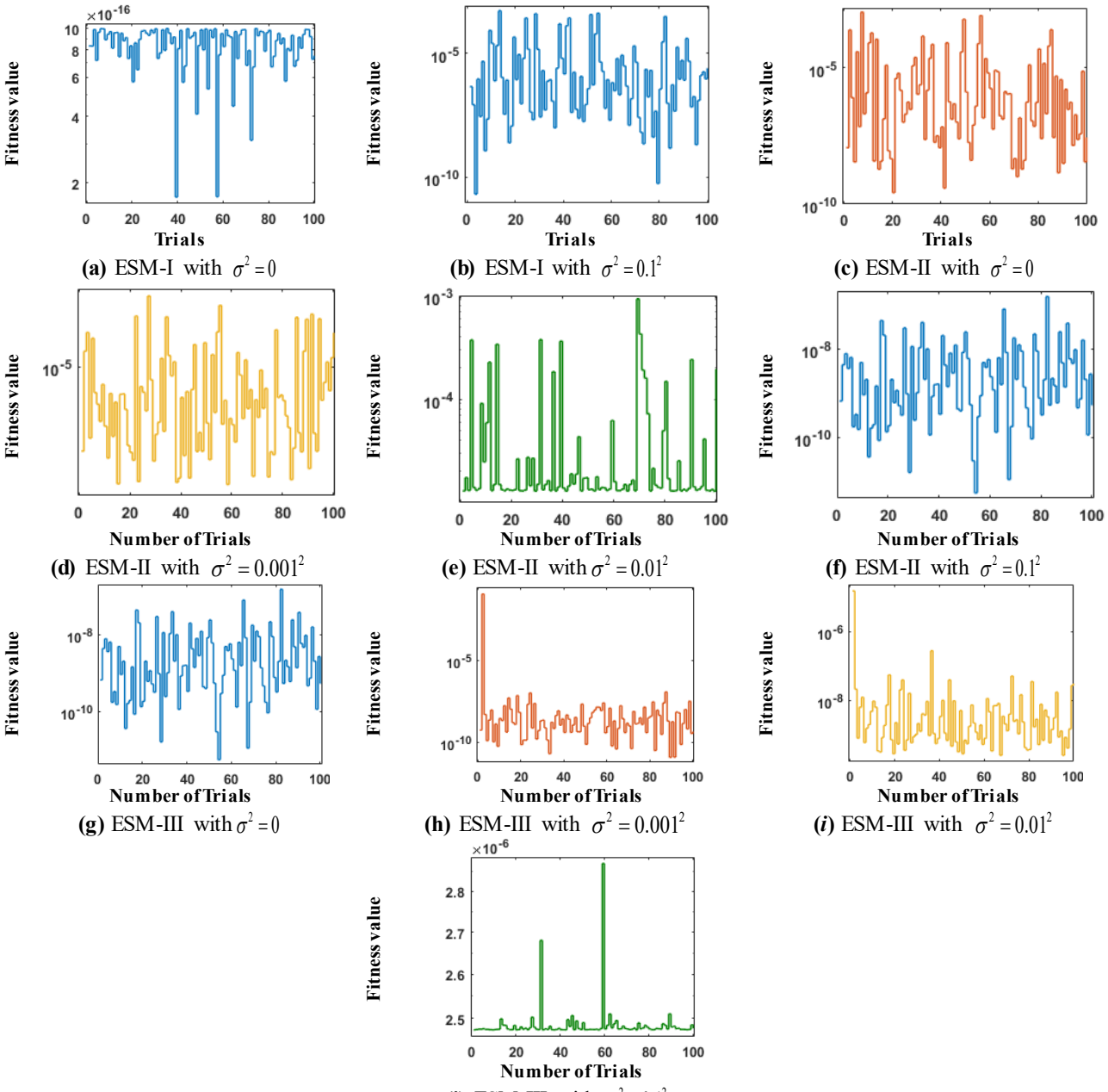

(a) ESM-I with $\sigma^2 = 0$ **(b)** ESM-I with $\sigma^2 = 0.1^2$ **(c)** ESM-II with $\sigma^2 = 0$

(d) ESM-II with $\sigma^2 = 0.001^2$ **(e)** ESM-II with $\sigma^2 = 0.01^2$ **(f)** ESM-II with $\sigma^2 = 0.1^2$

(g) ESM-III with $\sigma^2 = 0$ **(h)** ESM-III with $\sigma^2 = 0.001^2$ **(*i*)** ESM-III with $\sigma^2 = 0.01^2$

(j) ESM-III with $\sigma^2 = 0.1^2$

Fig. 9 Fitness plot for variants of ESM systems using DE

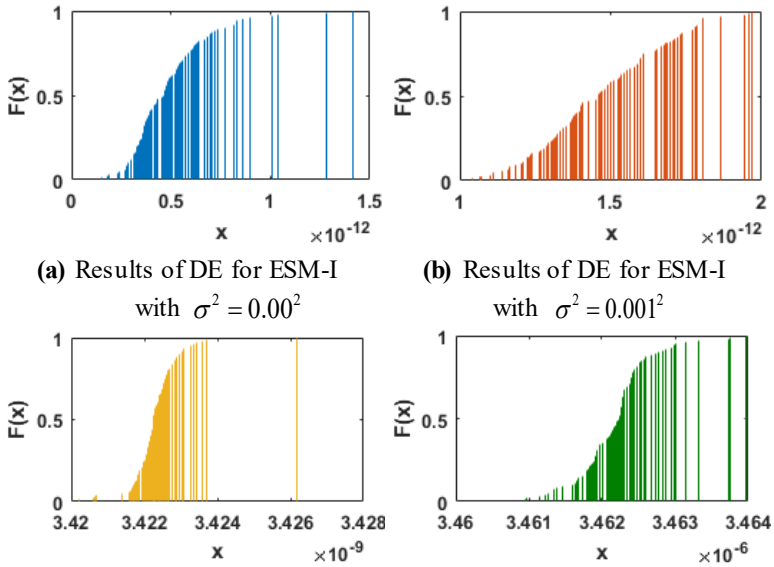

(a) Results of DE for ESM-I with $\sigma^2 = 0.00^2$

(b) Results of DE for ESM-I with $\sigma^2 = 0.001^2$

(c) Results of GAs for ESM-I with, $\sigma^2 = 0.01^2$

(d) Results of GAs for ESM-I with, $\sigma^2 = 0.1^2$

Fig. 10 Plots of TIC indices for variants of ESM-1 system

Table 5: Results of statistical operators for variants of ESM-III system

Solver	Noise	Model	Approximate Parameter Vector								
			$i=1$	$i=2$	$i=3$	$i=4$	$i=5$	$i=6$	$i=7$	$i=8$	$i=9$
DE	0.000^2	Best	-1.094	0.109	1.000	-0.249	-2.78E-02	1.90E-03	-7.83E-06	1.95E-08	2.36E-08
		Mean	-1.094	0.109	1.000	-0.249	-2.78E-02	1.90E-03	-7.83E-06	1.81E-08	2.36E-08
		Worst	-1.094	0.109	1.000	-0.249	-2.78E-02	1.90E-03	-7.83E-06	2.83E-08	2.36E-08
	0.001^2	Best	-1.094	0.109	1.000	-0.249	-2.78E-02	1.90E-03	-7.77E-06	2.29E-08	2.36E-08
		Mean	-1.094	0.109	1.000	-0.249	-2.78E-02	1.90E-03	-7.76E-06	2.91E-08	2.36E-08
		Worst	-1.094	0.109	1.000	-0.249	-2.78E-02	1.90E-03	-7.76E-06	3.49E-08	2.36E-08
	0.010^2	Best	-1.094	0.109	1.000	-0.249	-2.78E-02	1.90E-03	-1.24E-06	1.18E-06	2.36E-08
		Mean	-1.094	0.109	1.000	-0.249	-2.78E-02	1.90E-03	-1.24E-06	1.19E-06	2.36E-08
		Worst	-1.094	0.109	1.000	-0.249	-2.78E-02	1.90E-03	-1.25E-06	1.19E-06	2.36E-08
	0.100^2	Best	-1.095	0.109	1.000	-0.249	-2.78E-02	1.81E-03	6.51E-04	1.19E-04	2.33E-08
		Mean	-1.095	0.109	1.000	-0.249	-2.78E-02	1.81E-03	6.51E-04	1.19E-04	2.33E-08
		Worst	-1.095	0.109	1.000	-0.249	-2.78E-02	1.81E-03	6.51E-04	1.19E-04	2.33E-08
GAs	0.000^2	Best	-1.094	0.109	1.000	-0.249	-2.79E-02	1.93E-03	-1.29E-05	-1.22E-05	2.36E-08
		Mean	-1.094	0.109	1.000	-0.249	-2.78E-02	1.89E-03	-3.43E-06	4.60E-06	2.36E-08
		Worst	-1.094	0.109	1.000	-0.249	-2.73E-02	1.88E-03	2.43E-05	7.49E-06	2.34E-08
	0.001^2	Best	-1.094	0.109	1.000	-0.249	-2.77E-02	1.90E-03	-6.73E-07	1.19E-06	2.36E-08
		Mean	-1.094	0.109	0.990	-0.247	-2.78E-02	1.89E-03	-6.48E-06	1.86E-06	2.97E-05
		Worst	-1.094	0.109	1.000	-0.249	-2.78E-02	1.90E-03	1.03E-06	2.70E-06	2.36E-08
	0.010^2	Best	-1.094	0.109	1.000	-0.249	-2.76E-02	2.00E-03	2.52E-06	-2.85E-05	2.35E-08
		Mean	-1.094	0.109	1.000	-0.249	-2.79E-02	1.90E-03	-8.70E-06	1.64E-06	2.36E-08
		Worst	-1.094	0.109	1.000	-0.249	-2.78E-02	1.93E-03	-7.98E-06	-1.06E-05	2.36E-08
	0.100^2	Best	-1.094	0.109	1.000	-0.249	-2.78E-02	2.05E-03	1.90E-04	2.71E-05	2.33E-08
		Mean	-1.094	0.109	1.000	-0.249	-2.78E-02	2.04E-03	1.89E-04	3.21E-05	2.33E-08
		Worst	-1.000	0.800	1.000	2.799	-4.799	5.700	0.600	2.11E-05	2.78E-08
True Values			-1.000	0.800	1.000	2.800	-4.800	5.700	0.600	1.95E-08	2.36E-08

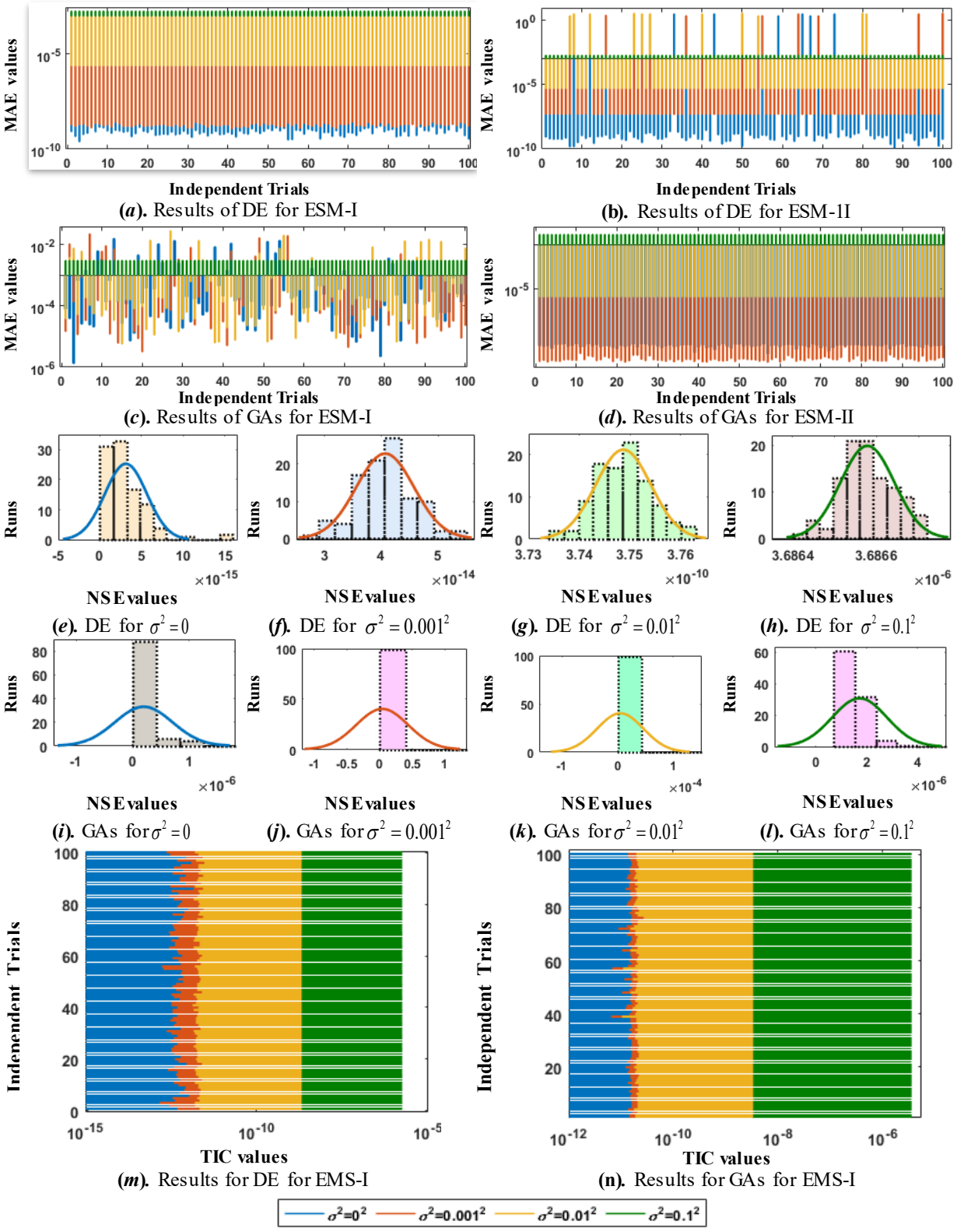

Fig. 11. Results based on MAE, NSE and TIC indices through bar, histogram and stack-bar graphics for ESM-I and II.

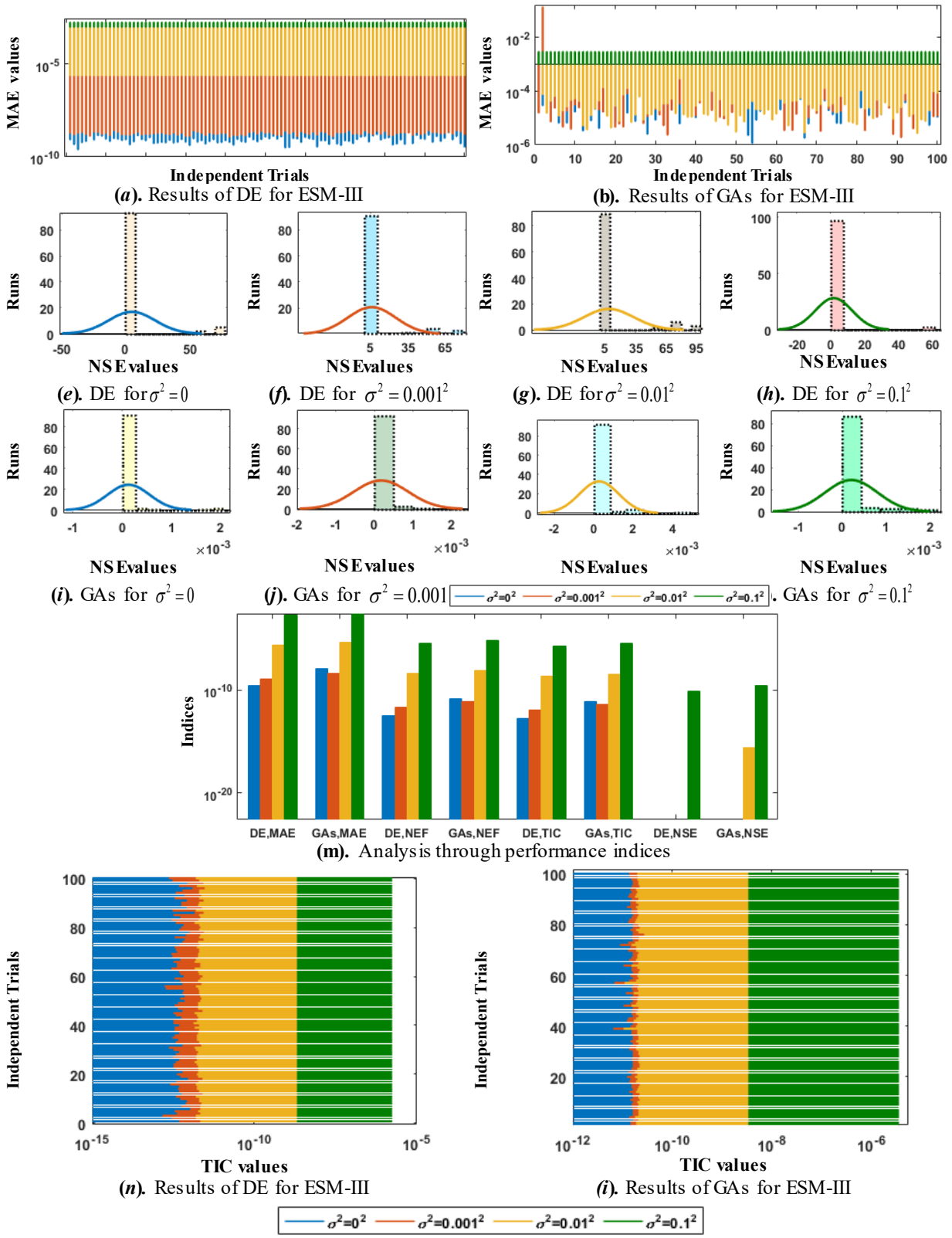

Fig. 12 Results based on MAE, NSE and TIC indices through bar, histogram, and stack-bar graphics for ESM-III.

Table 6: Statistical analysis on global operators for each case of all ESM models

Solver	ESM	Noise σ^2	Global Operators							
			Fitness ε		MWD δ		NSE		TIC	
			Mean	STD	Mean	STD	Mean	STD	Mean	STD
DE	I	0^2	1.13E-18	1.14E-18	8.19E-10	3.50E-10	0.00E+00	0.00E+00	4.99E-13	2.17E-13
		10^{-4}	3.34E-12	8.64E-19	1.81E-09	3.28E-10	0.00E+00	0.00E+00	1.47E-12	2.17E-13
		10^{-2}	3.34E-08	1.39E-18	2.40E-06	4.57E-10	0.00E+00	0.00E+00	2.05E-09	2.51E-13
		10^{-1}	1.83E-04	1.17E-18	1.87E-03	3.52E-10	7.33E-11	9.79E-17	1.75E-06	7.92E-14
	II	0^2	5.62E+00	2.06E+01	2.00E-01	7.40E-01	4.93E+00	1.82E+01	4.89E-02	1.79E-01
		10^{-4}	7.22E+00	2.49E+01	2.40E-01	7.82E-01	5.88E+00	1.94E+01	6.18E-02	1.99E-01
		10^{-2}	7.00E+00	2.20E+01	3.35E-01	9.69E-01	8.54E+00	2.48E+01	8.25E-02	2.38E-01
		10^{-1}	2.37E+00	1.36E+01	1.87E-03	3.52E-10	1.89E+00	1.09E+01	2.00E-02	1.14E-01
	III	0^2	1.59E-16	1.04E-16	6.68E-09	2.44E-09	3.12E-15	2.52E-15	8.97E-09	3.41E-09
		10^{-4}	3.13E-14	8.34E-17	2.46E-08	2.13E-09	4.07E-14	5.09E-15	3.45E-08	2.18E-09
		10^{-2}	3.12E-10	1.15E-16	2.13E-06	2.76E-09	3.75E-10	5.46E-13	3.32E-06	2.42E-09
		10^{-1}	3.12E-06	1.30E-16	1.87E-03	3.52E-10	3.69E-06	6.44E-11	3.29E-04	2.88E-09
GAs	I	0^2	8.42E-16	1.72E-16	2.35E-08	3.63E-09	0.00E+00	0.00E+00	1.48E-11	1.78E-12
		10^{-4}	7.57E-12	4.04E-17	6.00E-09	1.97E-09	0.00E+00	0.00E+00	5.02E-12	9.17E-13
		10^{-2}	7.56E-08	2.62E-17	4.19E-06	1.41E-09	2.22E-16	0.00E+00	3.42E-09	6.92E-13
		10^{-1}	4.01E-04	1.56E-10	3.04E-03	3.09E-06	2.87E-10	8.75E-14	3.46E-06	5.28E-10
	II	0^2	3.20E-05	9.38E-05	1.38E-03	3.23E-03	1.25E-04	4.26E-04	3.20E-04	7.44E-04
		10^{-4}	4.02E-05	1.47E-04	1.52E-03	3.82E-03	1.71E-04	7.02E-04	3.50E-04	8.78E-04
		10^{-2}	6.02E-05	2.17E-04	2.03E-03	4.76E-03	2.72E-04	9.96E-04	4.68E-04	1.10E-03
		10^{-1}	5.75E-05	1.25E-04	3.04E-03	3.09E-06	2.04E-04	5.96E-04	4.80E-04	9.14E-04
	III	0^2	7.68E-09	1.88E-08	3.20E-05	3.23E-05	1.97E-07	5.07E-07	5.24E-05	5.56E-05
		10^{-4}	1.18E-03	1.18E-02	1.42E-03	1.39E-02	3.97E-02	3.97E-01	4.01E-03	3.95E-02
		10^{-2}	1.57E-07	1.48E-06	5.21E-05	1.95E-04	4.38E-06	4.16E-05	8.77E-05	3.50E-04
		10^{-1}	2.49E-06	4.45E-08	3.04E-03	3.09E-06	1.72E-06	1.08E-06	2.20E-04	4.68E-05

Complexity of the designed schemes is determined in terms of time consumed for execution by each solver, cycles completed, function evaluated. Results based on these measures are obtained for 100 trials of each solver and are provided in Table 7 for mean and standard deviation measures. The values of mean execution time, generations and functions evaluations are close to 7.389 ± 0.45, 207.55 ± 1.45 and 37563.740± 7.45 for ESM-I, 9.839± 0.640, 182.6 ± 11.161 and 38527.6± 9.8 for ESM-II and 18.50 ± 0.8, 233.750 ± 6.28 and 63345.250 ± 18.438 for ESM-III in case of DE while the for GAs the respective magnitudes are around 11.161± 0.57, 300 and 60200 for ESM-I, 24.876± 0.3, 700 and 140200 for ESM-II and 21.334± 0.8, 500 and 100200 for ESM-III. It is seen that DE outperforms GAs in terms of each complexity operator based on execution time, generations consumed and functions evaluated. All numerical experimentations for ESM models are conducted on Dell notebook 35212, Intel Core(TM) i3, CPU @ 1.90 GHz processor and 6.00 GB of RAM.

Table 7: Results of complexity measures for all three ESM models

Solver	ESM	Noise σ^2	Complexity Operators					
			Time		Generations		Function Counts	
			Mean	STD	Mean	STD	Mean	STD
DE	I	0^2	7.362	0.595	208.540	14.082	37744.740	7.362
		10^{-4}	7.389	0.496	207.540	13.693	37563.740	7.389
		10^{-2}	7.524	0.531	209.260	14.385	37875.060	7.524
		10^{-1}	7.489	0.471	211.820	12.481	38338.420	7.489
	II	0^2	10.572	0.754	183.040	6.399	38620.440	10.572
		10^{-4}	9.839	0.640	182.600	11.161	38527.600	9.839
		10^{-2}	9.920	0.398	183.710	7.458	38761.810	9.920
		10^{-1}	10.058	0.697	182.170	6.495	38436.870	10.058
	III	0^2	21.638	17.654	234.720	6.529	63011.950	21.638
		10^{-4}	18.043	0.514	233.750	6.288	63345.250	18.043
		10^{-2}	17.899	0.762	233.790	5.661	63356.090	17.899
		10^{-1}	20.209	18.238	234.430	6.557	63529.530	20.209
GAs	I	0^2	10.369	0.000	214.010	26.558	60200.000	10.369
		10^{-4}	11.161	0.599	300.000	0.000	60200.000	11.161
		10^{-2}	9.723	0.282	300.000	0.000	60200.000	9.723
		10^{-1}	10.642	0.556	300.000	0.000	60200.000	10.642
	1I	0^2	24.679	0.971	700.000	0.000	140200.000	24.679
		10^{-4}	25.239	0.272	700.000	0.000	140200.000	25.239
		10^{-2}	24.876	0.284	700.000	0.000	140200.000	24.876
		10^{-1}	23.956	0.207	700.000	0.000	140200.000	23.956
	III	0^2	20.638	0.269	500.000	0.000	100200.000	20.638
		10^{-4}	21.334	0.134	500.000	0.000	100200.000	21.334
		10^{-2}	19.987	0.154	500.000	0.000	100200.000	19.987
		10^{-1}	21.012	0.184	500.000	0.000	100200.000	21.012

In order to compare the performance of the proposed DE with other state-of-the-art heuristics the results of DE are also compared with particle swarm optimization (PSO), simulated annealing (SA) and pattern search (PS) techniques. The results of PSO, SA and PS in terms of accuracy and complexity measures are listed in Table 8. It can be observed that the fitness values lie in the range of 10^{-04} to 10^{-10}, 10^{-03} to 10^{-04}, and 10^{-06} to 10^{-14} for ESM-I, ESM-II, and ESM-III, respectively, in case of PSO, while for PS respective values lie close to 10^{-04} to 10^{-9}, 10^{+01} to 10^{-04}, and 10^{-01} to 10^{-08}, whereas in case of SA respective magnitudes ranges between 10^{-01} to 10^{-02}, 10^{+01} to 10^{-01}, and 10^{+03} to 10^{-01}. Generally, good results in terms of accuracy are obtained by PSO while performance degraded considerably for PS and SA algorithms. However, PSO consumed more time and function counts than other two algorithms, hence PSO is considered more complex. Comparison of the results of PSO with DE and GAs, show that PSO achieve the similar accuracy as that of GAs but considerably `degraded performance of accuracy than that of DE. Moreover, the complexity of DE algorithm for optimization of decision variable is much better than that of GAs and PSO algorithms.

Table 8: Comparison of the performance on basis of best runs of all three algorithms for each variant of ESM models

Solver	ESM	σ^2	Accuracy					Complexity	
			ε	δ	MAE	NSE	TIC	Time	FC
PSO	I	0	4.08E-09	6.55E-08	5.43E-05	2.58E-14	3.27E-08	250.8	1600200
		10^{-3}	6.58E-10	6.55E-08	2.02E-05	4.00E-15	1.29E-08	212.1	1600200
		10^{-2}	2.04E-07	7.87E-08	3.65E-05	1.47E-14	2.48E-08	212.5	1600200
		10^{-1}	8.12E-04	7.87E-08	2.43E-03	1.77E-10	2.72E-06	214.1	1600200
	II	0	1.73E-04	6.55E-08	8.93E-03	8.59E-04	2.12E-03	571.5	4066493
		10^{-3}	2.45E-04	6.29E-07	1.06E-02	1.21E-03	2.52E-03	631.1	4000040
		10^{-2}	5.76E-04	6.28E-07	8.63E-03	7.96E-04	2.04E-03	639.4	4000040
		10^{-1}	1.30E-03	4.05E-07	2.43E-03	3.45E-04	1.34E-03	630.8	4000040
	III	0	0.00E+00	6.55E-08	0.00E+00	0.00E+00	0.00E+00	1926.5	10000100
		10^{-3}	1.90E-14	6.28E-07	4.12E-08	1.27E-13	6.12E-08	1885.3	10000100
		10^{-2}	1.90E-10	4.05E-07	4.12E-06	1.27E-09	6.12E-06	1900.9	10000100
		10^{-1}	1.90E-06	6.28E-07	2.43E-03	1.27E-05	6.12E-04	1932.2	10000100
PS	I	0	1.05E-09	3.33E-08	1.34E-05	6.66E-15	1.66E-08	7.20	2444
		10^{-3}	1.36E-11	4.60E-06	1.60E-06	0.00E+00	1.30E-09	8.19	2396
		10^{-2}	7.31E-08	1.39E-04	6.78E-06	4.44E-16	4.78E-09	8.19	2393
		10^{-1}	3.02E-04	7.12E-05	2.62E-03	2.09E-10	2.95E-06	8.28	3643
	II	0	3.69E-04	1.12E-06	7.46E-03	5.53E-04	1.70E-03	11.63	4165
		10^{-4}	2.81E-03	2.24E-06	2.40E-02	5.68E-03	5.47E-03	11.60	4263
		10^{-2}	1.05E-03	1.38E-05	1.37E-02	1.84E-03	3.10E-03	11.56	4489
		10^{-1}	1.88E+01	7.12E-05	2.62E-03	9.47E+01	8.80E-01	11.43	5032
	III	0	8.33E-08	4.45E-06	1.30E-04	1.97E-06	2.41E-04	11.90	5502
		10^{-4}	8.22E-08	7.33E-06	1.40E-04	2.07E-06	2.47E-04	12.73	5712
		10^{-2}	1.53E-07	3.31E-06	1.84E-04	3.82E-06	3.35E-04	12.93	6286
		10^{-1}	2.46E-01	7.12E-05	2.62E-03	6.91E+00	4.94E-01	13.14	6365
SA	I	0	1.63E-02	1.31E-04	8.62E-02	1.02E-07	6.54E-05	2.99	18001
		10^{-3}	1.67E-01	1.31E-04	3.26E-01	1.05E-06	2.09E-04	2.78	16860
		10^{-2}	6.03E-02	6.59E-04	2.21E-01	3.79E-07	1.26E-04	4.17	16650
		10^{-1}	4.95E-02	6.59E-04	1.62E-01	8.28E-07	1.86E-04	3.41	18001
	II	0	1.26E+01	1.31E-04	1.79E+00	3.00E+01	4.92E-01	3.56	19110
		10^{-3}	2.93E+01	4.60E-04	1.89E+00	3.41E+01	5.08E-01	3.87	19576
		10^{-2}	1.31E+01	2.59E-04	1.95E+00	3.53E+01	5.19E-01	4.01	20878
		10^{-1}	2.28E+00	1.55E-04	1.62E-01	3.15E+01	5.07E-01	4.80	21000
	III	0	1.77E+01	1.31E-04	1.17E+00	6.74E+01	8.10E-01	4.92	21060
		10^{-3}	1.03E+03	2.59E-04	3.00E+00	4.68E+02	8.48E-01	5.10	22534
		10^{-2}	6.66E+01	1.55E-04	1.32E+00	2.30E+02	8.61E-01	5.56	24378
		10^{-1}	1.09E+01	2.59E-04	1.62E-01	7.48E+01	7.33E-01	5.94	24989

The analysis of accuracy level of PSO, PS and SA is further conducted on the basis of 100 independent executions of each algorithm for optimization of decision variable of EMS models. Results of statistics in terms of best, mean and worst indices are given in Table 9 for ESM-I along with the desired parameters, while, the results for ESM-II and ESM-III are provided in Tables 10 and 11 respectively, for each scenarios. It is observed that with the increase in noise level $\sigma^2 = 0.001^2$ to 0.1^2 degradation in the performance is noticed in case of both PSO and PS, however,

both the algorithms are significantly applicable for finding the optimal ESM parameters with reasonable accuracy, while the results of SA are relatively poor. Comparing the performance with proposed DE algorithm, it can be evidently seen that performance of PSO is almost similar to GAs, but relative better that PS and SA algorithms, however inferior than that of DE based method.

Table 9: Comparison through results of statistics for variants of ESM-I system

Solver	σ^2	Model	Approximate Parameter Vector					
			$i=1$	$i=2$	$i=3$	$i=4$	$i=5$	$i=6$
PSO	0^2	Best	-1.998	0.998	0.002	6.899	0.041	2389.7
		Mean	-1.999	0.998	0.002	6.899	0.041	2389.7
		Worst	-1.998	0.998	0.003	6.900	0.041	2389.7
	10^{-4}	Best	-1.998	0.999	0.002	6.899	0.041	2389.7
		Mean	-1.999	0.999	0.002	6.899	0.041	2389.7
		Worst	-2.000	0.998	0.002	6.899	0.041	2389.7
	10^{-2}	Best	-1.999	0.998	0.002	6.899	0.041	2389.7
		Mean	-1.999	0.998	0.002	6.899	0.041	2389.7
		Worst	-2.000	0.998	0.002	6.899	0.041	2389.7
	10^{-1}	Best	-2.000	0.986	0.002	6.899	0.041	2389.7
		Mean	-2.000	0.986	0.002	6.899	0.041	2389.7
		Worst	-2.000	0.986	0.002	6.899	0.041	2389.7
SA	0^2	Best	-1.956	0.936	-0.080	6.869	0.094	2389.7
		Mean	-1.718	1.003	0.061	6.681	0.029	2389.7
		Worst	-1.332	0.091	0.730	5.867	-0.632	2389.3
	10^{-4}	Best	-1.940	1.139	0.012	6.801	-0.050	2389.7
		Mean	-1.717	1.027	0.023	6.736	0.041	2389.6
		Worst	-0.929	0.685	0.762	6.391	-0.625	2389.5
	10^{-2}	Best	-1.813	1.003	0.022	6.929	0.070	2389.6
		Mean	-1.682	0.995	-0.029	6.674	0.082	2389.7
		Worst	-1.033	1.633	0.528	6.494	0.677	2389.6
	10^{-1}	Best	-1.919	1.091	-0.026	6.883	-0.021	2389.8
		Mean	-1.670	0.990	0.015	6.665	0.101	2389.7
		Worst	-1.640	1.585	0.140	6.103	1.434	2388.8
PS	0^2	Best	-1.998	0.999	0.002	6.899	0.041	2389.7
		Mean	-1.968	1.002	0.019	6.900	0.048	2389.7
		Worst	-1.999	0.993	0.642	6.898	0.039	2389.7
	10^{-4}	Best	-1.999	0.999	0.002	6.899	0.041	2389.7
		Mean	-1.941	1.004	0.015	6.900	0.068	2389.7
		Worst	-0.438	0.994	-0.002	6.886	0.036	2389.7
	10^{-2}	Best	-1.999	0.999	0.002	6.899	0.041	2389.7
		Mean	-1.952	1.005	0.030	6.900	0.060	2389.7
		Worst	-1.999	0.996	-0.002	6.897	1.253	2389.6
	10^{-1}	Best	-2.000	0.984	0.002	6.899	0.041	2389.7
		Mean	-1.918	0.988	0.021	6.898	0.063	2389.7
		Worst	-0.788	0.995	-0.017	6.873	0.030	2389.7
True Parameter Vector			-1.998	0.998	0.002	6.899	0.041	2389.7

Table 10: Comparison through results of statistics for variants of ESM-II system

Solver	Noise	Model	Approximate Parameter Vector						
			$i=1$	$i=2$	$i=3$	$i=4$	$i=5$	$i=6$	$i=7$
PSO	0.000^2	Best	-1.000	0.800	1.004	2.790	-4.779	5.675	0.603
		Mean	-1.000	0.800	1.044	2.701	-4.600	5.456	0.627
		Worst	-1.000	0.800	1.108	2.563	-4.326	5.125	0.666
	0.001^2	Best	-1.000	0.800	1.005	2.788	-4.775	5.670	0.603
		Mean	-1.000	0.800	1.081	2.639	-4.457	5.284	0.650
		Worst	-1.000	0.800	1.219	2.371	-3.923	4.635	0.736
	0.010^2	Best	-1.000	0.800	1.004	2.790	-4.782	5.674	0.602
		Mean	-1.000	0.800	1.027	2.740	-4.675	5.546	0.617
		Worst	-1.000	0.800	1.081	2.624	-4.440	5.259	0.649
	0.100^2	Best	-1.000	0.800	1.012	2.777	-4.743	5.630	0.607
		Mean	-1.000	0.800	1.026	2.745	-4.681	5.554	0.616
		Worst	-1.000	0.800	1.101	2.585	-4.356	5.158	0.662
SA	0.000^2	Best	-1.040	0.808	4.029	1.379	-1.413	1.361	0.905
		Mean	-0.989	0.799	1.830	1.158	-1.380	1.679	1.293
		Worst	-1.067	0.836	1.515	-3.593	-3.352	5.871	1.299
	0.001^2	Best	-1.073	0.809	4.511	1.950	-1.345	1.036	-0.067
		Mean	-0.986	0.796	1.409	1.002	-1.326	1.657	1.001
		Worst	-0.955	0.783	3.171	2.179	-1.228	1.099	2.020
	0.010^2	Best	-1.019	0.799	4.487	1.571	-1.200	1.025	1.229
		Mean	-0.982	0.794	1.464	1.250	-1.418	1.687	0.917
		Worst	-0.918	0.779	-3.361	-1.170	0.849	-1.036	-4.169
	0.100^2	Best	-0.985	0.795	1.734	2.008	-2.573	2.994	1.137
		Mean	-0.979	0.792	1.586	1.242	-1.146	1.269	1.126
		Worst	-0.959	0.788	2.605	0.589	-1.482	1.997	2.822
PS	0.000^2	Best	-0.999	0.799	1.004	2.794	-4.781	5.682	0.604
		Mean	-1.020	0.826	-0.782	1.293	-2.050	2.549	-0.475
		Worst	-1.007	0.809	-3.577	-0.771	1.338	-1.536	-2.109
	0.001^2	Best	-0.999	0.799	1.013	2.777	-4.740	5.641	0.610
		Mean	-1.032	0.840	-0.639	1.322	-2.047	2.544	-0.451
		Worst	-1.548	1.459	0.443	-4.944	-0.606	-4.997	0.491
	0.010^2	Best	-0.999	0.799	1.008	2.787	-4.765	5.667	0.606
		Mean	-1.009	0.811	-0.587	1.421	-2.477	2.943	-0.289
		Worst	-1.007	0.809	-3.577	-0.771	1.338	-1.536	-2.109
	0.100^2	Best	-1.007	0.809	-3.577	-0.771	1.338	-1.536	-2.108
		Mean	-1.030	0.836	-1.030	1.218	-1.692	2.251	-0.582
		Worst	-1.007	0.809	-3.577	-0.771	1.338	-1.536	-2.108
True Values			-1.000	0.800	1.000	2.800	-4.800	5.700	0.600

Table 11: Comparison through results of statistics for variants of ESM-III system

Solver	Noise	Model	Approximate Parameter Vector								
			$i=1$	$i=2$	$i=3$	$i=4$	$i=5$	$i=6$	$i=7$	$i=8$	$i=9$
DE	0.000^2	Best	-1.094	0.109	1.000	-0.249	-0.028	0.002	-7.83E-06	1.78E-08	2.36E-08
		Mean	-1.094	0.109	1.000	-0.249	-0.028	0.002	-7.83E-06	1.78E-08	2.36E-08
		Worst	-1.094	0.109	1.000	-0.249	-0.028	0.002	-7.83E-06	1.78E-08	2.36E-08
	0.001^2	Best	-1.094	0.109	1.000	-0.249	-0.028	0.002	-7.84E-06	-6.94E-08	2.36E-08
		Mean	-1.094	0.109	1.000	-0.249	-0.028	0.002	-7.84E-06	-6.94E-08	2.36E-08
		Worst	-1.094	0.109	1.000	-0.249	-0.028	0.002	-7.84E-06	-6.94E-08	2.36E-08
	0.010^2	Best	-1.094	0.109	1.000	-0.249	-0.028	0.002	-9.12E-06	-8.70E-06	2.36E-08
		Mean	-1.094	0.109	1.000	-0.249	-0.028	0.002	-9.12E-06	-8.70E-06	2.36E-08
		Worst	-1.094	0.109	1.000	-0.249	-0.028	0.002	-9.12E-06	-8.70E-06	2.36E-08
	0.100^2	Best	-1.095	0.108	1.000	-0.249	-0.028	0.003	-1.37E-04	-8.73E-04	2.36E-08
		Mean	-1.095	0.108	1.000	-0.249	-0.028	0.003	-1.37E-04	-8.73E-04	2.36E-08
		Worst	-1.095	0.108	1.000	-0.249	-0.028	0.003	-1.37E-04	-8.73E-04	2.36E-08
GAs	0.000^2	Best	0.851	-0.361	0.694	2.380	1.413	1.160	1.68E+00	-8.88E-01	-8.65E-07
		Mean	0.422	0.800	0.286	-0.210	0.316	0.637	4.78E-01	7.50E-01	2.39E-01
		Worst	0.851	-0.361	0.694	2.380	1.413	1.160	1.68E+00	-8.88E-01	-8.65E-07
	0.001^2	Best	5.909	-1.676	5.945	2.561	0.814	-4.149	4.69E+00	8.09E-01	-1.58E-06
		Mean	0.473	0.101	0.186	-0.015	0.784	0.296	5.76E-01	1.61E+00	5.24E-02
		Worst	-2.805	-0.157	-4.276	-3.841	-2.976	2.560	5.43E+00	1.69E+00	-4.82E-07
	0.010^2	Best	1.649	1.025	1.419	-1.454	1.329	1.251	-1.57E+00	2.42E+00	3.22E-05
		Mean	0.256	0.530	0.008	0.123	0.686	0.268	6.12E-01	-4.37E-01	-1.55E-02
		Worst	0.470	0.790	-0.217	1.213	1.374	1.432	6.25E-01	7.92E-01	-1.84E-07
	0.100^2	Best	3.247	-0.798	2.903	-2.901	-1.623	-1.754	9.44E-01	3.55E-01	-1.95E-05
		Mean	0.308	0.662	-0.024	0.105	0.389	0.333	1.27E-01	1.64E+00	5.92E-03
		Worst	0.691	4.288	0.546	-0.553	4.499	2.280	-3.39E+00	2.87E+00	5.49E-05
DE	0.000^2	Best	-1.094	0.109	1.000	-0.249	-0.027	0.002	1.02E-04	-8.83E-06	2.33E-08
		Mean	-1.093	0.110	0.097	-0.037	-0.028	-0.214	-9.10E-03	-1.41E-01	-8.49E-06
		Worst	-0.906	0.267	-0.681	0.681	-0.028	-5.115	-1.37E-01	-1.61E+00	-1.27E-04
	0.001^2	Best	-1.094	0.109	1.000	-0.249	-0.027	0.002	1.01E-04	-8.84E-06	2.33E-08
		Mean	-1.095	0.108	0.152	-0.085	-0.028	-0.254	-1.34E-02	-1.72E-01	-1.11E-05
		Worst	-0.965	0.216	-0.663	0.663	-0.028	-3.408	-9.60E-02	-1.12E+00	-8.63E-05
	0.010^2	Best	-1.094	0.109	1.000	-0.249	-0.027	0.002	9.67E-05	-9.73E-06	2.32E-08
		Mean	-1.090	0.112	0.056	-0.019	-0.028	-0.365	-1.39E-02	-2.10E-01	-1.19E-05
		Worst	-0.955	0.224	-0.559	0.559	-0.028	-3.498	-1.28E-01	-1.49E+00	-1.01E-04
	0.100^2	Best	-1.092	0.109	-0.173	0.173	-0.028	-0.337	-2.13E-02	-4.24E-01	-2.87E-05
		Mean	-1.087	0.114	0.066	-0.021	-0.029	-0.285	-8.76E-03	-1.83E-01	-1.26E-05
		Worst	-1.017	0.170	-0.409	0.409	-0.028	-1.699	-8.96E-02	-1.10E+00	-6.33E-05
True Values			-1.094	0.109	1.000	-0.249	-0.028	0.002	-7.83E-06	1.78E-08	2.36E-08

The performance of the DE approach for ESM models is also investigated through single objective based merit function given in (18) and results in terms of the learning curves are given in Fig. 13. While, the detailed evaluation of the accuracy of the algorithm using single objective based merit function given in (18) is carried out by statistical performance measures of mean, best, and worst magnitudes of the estimated parameters and results are presented in Tables 12, 13 and 14 for ESM-I, ESM-II and ESM-III respectively. It is seen from the convergence plots presented in Fig. 13 that minimum error in the responses of the ESM models I, II and III can be achieved by using objective

function (18) but convergence to the desired parameters is not guaranteed as can be seen from Tables 12 to 14 for ESM-I, ESM-II and ESM-III respectively.

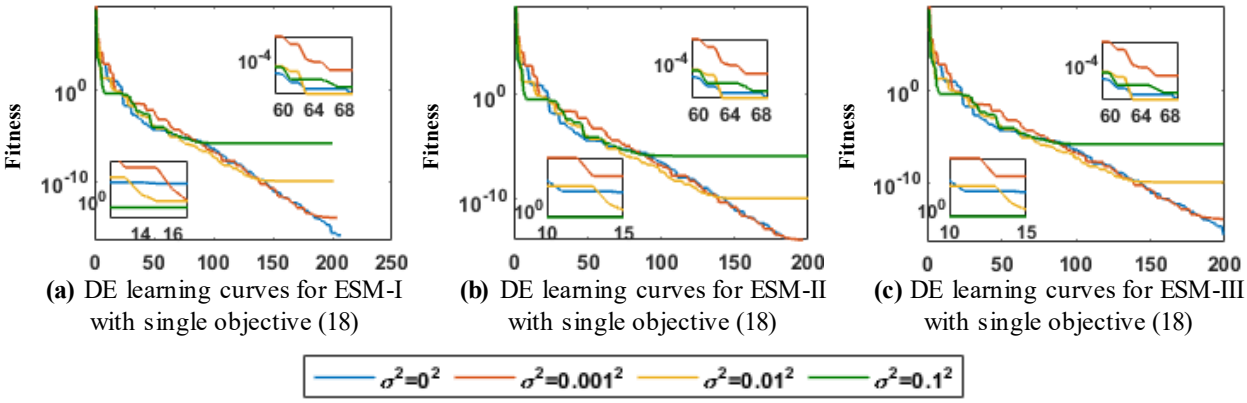

(a) DE learning curves for ESM-I with single objective (18)

(b) DE learning curves for ESM-II with single objective (18)

(c) DE learning curves for ESM-III with single objective (18)

Fig. 13. Results for iterative adaptation using single objective based merit function of ESM-I, II and III

Table 12: Comparison through statistical results for variants of ESM-I system using single objective based merit function

Solver	σ^2	Model	Approximate Parameter Vector					
			$i=1$	$i=2$	$i=3$	$i=4$	$i=5$	$i=6$
DE	0^2	Best	-1.493	0.383	-0.001	0.237	-0.012	6.774
		Mean	-0.869	0.586	-0.015	0.028	0.000	3.395
		Worst	1.529	1.349	-0.008	0.028	0.000	1.837
	10^{-4}	Best	-1.743	0.679	0.017	-0.006	-0.047	9.804
		Mean	-0.855	0.615	-0.002	-0.004	-0.080	2.253
		Worst	1.521	1.099	-0.035	0.000	-0.859	-0.950
	10^{-2}	Best	-2.288	1.342	0.155	0.399	0.024	79.459
		Mean	-1.314	0.698	-0.046	0.049	-0.158	9.897
		Worst	-0.237	-1.056	-0.018	0.001	-0.197	-0.970
	10^{-1}	Best	-1.958	0.940	-0.013	0.224	-0.911	1.423
		Mean	-1.750	1.161	0.001	0.138	3.063	1.228
		Worst	-0.130	-1.214	-0.044	0.038	10.191	-3.005
True Parameter Vector			-1.998	0.998	0.002	6.899	0.041	2389.700

Table 13: Comparison through statistical results for variants of ESM-II system using single objective based merit function

Solver	Noise	Model	Approximate Parameter Vector						
			$i=1$	$i=2$	$i=3$	$i=4$	$i=5$	$i=6$	$i=7$
DE	0.000^2	Best	0.000	0.383	-0.001	0.237	-0.012	6.774	0.774
		Mean	-0.869	0.586	-0.015	0.028	0.000	3.395	1.321
		Worst	1.529	1.349	-0.008	0.028	0.000	1.837	-1.363
	0.001^2	Best	-1.743	0.679	0.017	-0.006	-0.047	9.804	0.880
		Mean	-0.855	0.615	-0.002	-0.004	-0.080	2.253	1.450
		Worst	1.521	1.099	-0.035	0.000	-0.859	-0.950	2.372
	0.010^2	Best	-2.288	1.342	0.155	0.399	0.024	79.459	1.068
		Mean	-1.314	0.698	-0.046	0.049	-0.158	9.897	1.868
		Worst	-0.237	-1.056	-0.018	0.001	-0.197	-0.970	2.787
	0.100^2	Best	-1.958	0.940	-0.013	0.224	-0.911	1.423	1.106
		Mean	-1.750	1.161	0.001	0.138	3.063	1.228	1.442
		Worst	-0.130	-1.214	-0.044	0.038	10.191	-3.005	2.122
True Values			-1.000	0.800	1.000	2.800	-4.800	5.700	0.600

Table 14: Comparison through statistical results for variants of ESM-III system using single objective based merit function

Solver	Noise	Model	Approximate Parameter Vector								
			$i=1$	$i=2$	$i=3$	$i=4$	$i=5$	$i=6$	$i=7$	$i=8$	$i=9$
DE	0.000^2	Best	-1.094	0.109	-0.004	0.001	4.621	-0.454	1.73E-03	-5.09E-06	-5.51E-06
		Mean	-1.094	0.110	-0.170	0.170	-5730.349	114.328	-7.63E-01	1.69E-03	1.69E-03
		Worst	-1.098	0.113	-1.695	1.697	-57575.591	1151.848	-7.68E+00	1.70E-02	1.71E-02
	0.001^2	Best	-1.094	0.109	0.002	-0.001	3.090	0.501	-1.28E-03	2.05E-05	5.52E-06
		Mean	-1.094	0.110	-0.221	0.221	-85680.575	1713.603	-1.14E+01	2.54E-02	2.54E-02
		Worst	-1.098	0.113	-2.204	2.207	-857185.653	17144.022	-1.14E+02	2.54E-01	2.54E-01
	0.010^2	Best	-1.094	0.109	0.001	0.000	2.768	1.279	3.86E-03	3.52E-03	1.47E-05
		Mean	-1.094	0.110	-0.131	0.131	0.016	-323.224	2.16E+00	-3.34E-03	-4.79E-03
		Worst	-1.098	0.113	-1.308	1.309	0.016	-3236.617	2.16E+01	-4.80E-02	-4.79E-02
	0.100^2	Best	-1.086	0.106	0.002	0.002	-0.094	18.973	-8.10E-02	-2.64E-01	2.82E-04
		Mean	-1.086	0.106	0.000	0.000	-0.014	3.070	3.31E-02	-3.11E-01	4.64E-05
		Worst	-1.086	0.106	0.001	0.001	-0.098	2.283	7.20E-02	-5.06E-01	3.53E-05
True Values			-1.094	0.109	1.000	-0.249	-0.028	0.002	-7.83E-06	1.78E-08	2.36E-08

6. Conclusions

Evolutionary computing paradigm based on DE is exploited as an accurate, reliable, robust and efficient tool for parameter estimation of Hammerstein systems in ESM model representing the scenarios of rehabilitation of the stroke patients. Hammerstein control autoregressive structure of ESM systems based on nonlinear characteristics of polynomial, sigmoid and spline kernels. Optimization strength of DE is employed for three ESM case studies for noiseless and noisy scenarios having variance $\sigma^2 = 0.001^2, 0.01^2,$ and 0.1^2. Comparative study of the proposed method from GAs, PSO, PS and SA based on performance metrics of MAE_ϑ, $ENSE_\vartheta$ and TIC_ϑ demonstrated the efficacy of DE in each scenarios of ESM models, while, the accuracy of estimation of both algorithm degraded for higher noise variances, but still the DE outperformed its

counterpart GA, PSO, PS and SA in terms of accuracy and complexity measures. Statistical observations further verify and validate the worth of DE over its counterparts for each scenario of ESM model.

One may explore in meta-heuristics of backtracking search optimization, weighted differential evolutions, fireworks, firefly, grey wolf optimizer, covariance matrix adaptation evolution strategy and improved environmental adaptation method for better identification of ESM models.

References

[1] Castro, M. J., Apple Jr, D. F., Hillegass, E. A., & Dudley, G. A. (1999). Influence of complete spinal cord injury on skeletal muscle cross-sectional area within the first 6 months of injury. European Journal of Applied Physiology and Occupational Physiology, 80(4), 373-378.

[2] Vestergaard, P., Krogh, K., Rejnmark, L., & Mosekilde, L. (1998). Fracture rates and risk factors for fractures in patients with spinal cord injury. Spinal cord, 36(11), 790.

[3] Mahoney, E. T., Bickel, C. S., Elder, C., Black, C., Slade, J. M., Apple, D., & Dudley, G. A. (2005). Changes in skeletal muscle size and glucose tolerance with electrically stimulated resistance training in subjects with chronic spinal cord injury. Archives of physical medicine and rehabilitation, 86(7), 1502-1504.

[4] Shields, R. K., & Dudley-Javoroski, S. (2007). Musculoskeletal adaptations in chronic spinal cord injury: effects of long-term soleus electrical stimulation training. Neurorehabilitation and neural repair, 21(2), 169-179.

[5] Howlett, O. A., Lannin, N. A., Ada, L., & McKinstry, C. (2015). Functional electrical stimulation improves activity after stroke: a systematic review with meta-analysis. *Archives of physical medicine and rehabilitation*, *96*(5), 934-943.

[6] Haeufle, D. F. B., Günther, M., Bayer, A., & Schmitt, S. (2014). Hill-type muscle model with serial damping and eccentric force–velocity relation. *Journal of biomechanics*, *47*(6), 1531-1536.

[7] Law, L. F., & Shields, R. K. (2007). Mathematical models of human paralyzed muscle after long-term training. Journal of biomechanics, 40(12), 2587-2595.

[8] Ding, J., Wexler, A. S., & Binder-Macleod, S. A. (2003). Mathematical models for fatigue minimization during functional electrical stimulation. Journal of Electromyography and Kinesiology, 13(6), 575-588.

[9] Hunt, K. J., Munih, M., Donaldson, N. D. N., & Barr, F. M. (1998). Investigation of the Hammerstein hypothesis in the modeling of electrically stimulated muscle. IEEE Transactions on Biomedical Engineering, 45(8), 998-1009.

[10] Bai, E. W., Cai, Z., Dudley-Javorosk, S., & Shields, R. K. (2009). Identification of a modified Wiener–Hammerstein system and its application in electrically stimulated paralyzed skeletal muscle modeling. Automatica, 45(3), 736-743.

[11] Le, F. (2011). Identification of electrically stimulated muscle after stroke Doctoral dissertation, University of Southampton.

[12] Le, F., Markovsky, I., Freeman, C. T., & Rogers, E. (2012). Recursive identification of Hammerstein systems with application to electrically stimulated muscle. Control Engineering Practice, 20(4), 386-396.

[13] Mehmood, A., Zameer, A., Chaudhary, N. I., & Raja, M. A. Z. (2019). Backtracking search heuristics for identification of electrical muscle stimulation models using Hammerstein structure. *Applied Soft Computing*, *84*, 105705.

[14] Greblicki, W., & Pawlak, M. (2017). Hammerstein system identification with the nearest neighbor algorithm. *IEEE Transactions on Information Theory*, *63*(8), 4746-4757.

[15] Castro-Garcia, R., Agudelo, O. M., & Suykens, J. A. (2017). Impulse response constrained LS-SVM modelling for MIMO Hammerstein system identification. *International Journal of Control*, 1-18.

[16] Giordano, G., Gros, S., & Sjöberg, J. (2018). An improved method for Wiener–Hammerstein system identification based on the Fractional Approach. *Automatica*, *94*, 349-360.

[17] Wang, D. (2016). Hierarchical parameter estimation for a class of MIMO Hammerstein systems based on the reframed models. *Applied Mathematics Letters*, *57*, 13-19..

[18] Chen, H., & Ding, F. (2015). Hierarchical least squares identification for Hammerstein nonlinear controlled autoregressive systems. Circuits, Systems, and Signal Processing, 34(1), 61-75.

[19] Mao, Y., Ding, F., & Yang, E. (2017). Adaptive filtering-based multi-innovation gradient algorithm for input nonlinear systems with autoregressive noise. International Journal of Adaptive Control and Signal Processing, 31(10), 1388-1400.

[20] Mao, Y., & Ding, F. (2015). Multi-innovation stochastic gradient identification for Hammerstein controlled autoregressive autoregressive systems based on the filtering technique. *Nonlinear Dynamics*, *79*(3), 1745-1755.

[21] Ding, F., Wang, F., Xu, L., Hayat, T., & Alsaedi, A. (2016). Parameter estimation for pseudo-linear systems using the auxiliary model and the decomposition technique. *IET Control Theory & Applications*, *11*(3), 390-400.

[22] Mao, Y., & Ding, F. (2016). A novel parameter separation based identification algorithm for Hammerstein systems. Applied Mathematics Letters, 60, 21-27.

[23] Chaudhary, N. I., et al., (2015). Design of fractional adaptive strategy for input nonlinear Box–Jenkins systems. Signal Processing, 116, 141-151.

[24] Chaudhary, N. I., et al., (2015). Design of modified fractional adaptive strategies for Hammerstein nonlinear control autoregressive systems. Nonlinear Dynamics, 82(4), 1811-1830.

[25] Cheng, S., Wei, Y., Sheng, D., Chen, Y., & Wang, Y. (2018). Identification for Hammerstein nonlinear ARMAX systems based on multi-innovation fractional order stochastic gradient. Signal Processing, 142, 1-10.

[26] Chaudhary, N. I., et al., (2015). Identification of Hammerstein nonlinear ARMAX systems using nonlinear adaptive algorithms. Nonlinear Dynamics, 79(2), 1385-1397.

[27] Aslam, M. S., et al., (2017). A sliding-window approximation-based fractional adaptive strategy for Hammerstein nonlinear ARMAX systems. Nonlinear Dynamics, 87(1), 519-533.

[28] Chaudhary, N. I., et al., (2017). Modified Volterra LMS algorithm to fractional order for identification of Hammerstein non-linear system. IET Signal Processing, 11(8), 975-985.

[29] Djenouri, Y., Belhadi, A., & Belkebir, R. (2018). Bees swarm optimization guided by data mining techniques for document information retrieval. *Expert Systems With Applications*, *94*, 126-136.

[30] Dhiman, G., & Kumar, V. (2018). Emperor Penguin Optimizer: A Bio-inspired Algorithm for Engineering Problems. *Knowledge-Based Systems*.

[31] Bose, D., Biswas, S., Vasilakos, A. V., & Laha, S. (2014). Optimal filter design using an improved artificial bee colony algorithm. *Information Sciences*, *281*, 443-461.

[32] Abiyev, R. H., & Tunay, M. (2015). Optimization of high-dimensional functions through hypercube evaluation. *Computational intelligence and neuroscience*, *2015*, 17.

[33] Zhao, W., Wang, L., & Zhang, Z. (2018). Atom search optimization and its application to solve a hydrogeologic parameter estimation problem. *Knowledge-Based Systems*.

[34] Chen, X., Mei, C., Xu, B., Yu, K., & Huang, X. (2018). Quadratic interpolation based teaching-learning-based optimization for chemical dynamic system optimization. *Knowledge-Based Systems*, *145*, 250-263.

[35] Lodhi, S., et al., 2019. Fractional neural network models for nonlinear Riccati systems. *Neural Computing and Applications*, *31*(1), pp.359-378.

[36] Kumar, A. and Kumar, V., 2018. Performance analysis of optimal hybrid novel interval type-2 fractional order fuzzy logic controllers for fractional order systems. *Expert Systems with Applications*, *93*, pp.435-455.

[37] Raja, M. A. Z., Abbas, S., Syam, M. I., & Wazwaz, A. M. (2018). Design of neuro-evolutionary model for solving nonlinear singularly perturbed boundary value problems. *Applied Soft Computing*, *62*, 373-394.

[38] Raja, M. A. Z. (2014). Numerical treatment for boundary value problems of pantograph functional differential equation using computational intelligence algorithms. *Applied Soft Computing*, *24*, 806-821.

[39] Umar, M., et al., 2019. Intelligent computing for numerical treatment of nonlinear prey–predator models. *Applied Soft Computing*, *80*, pp.506-524.

[40] Wang, Y., Feng, X., Lyu, X., Li, Z. and Liu, B., 2016. Optimal targeting of nonlinear chaotic systems using a novel evolutionary computing strategy. *Knowledge-Based Systems*, *107*, pp.261-270.

[41] Chen, K., Zhou, F. and Liu, A., 2018. Chaotic dynamic weight particle swarm optimization for numerical function optimization. *Knowledge-Based Systems*, *139*, pp.23-40.

[42] Ahmad, I., et al., (2018). Neuro-evolutionary computing paradigm for Painlevé equation-II in nonlinear optics. *The European Physical Journal Plus*, *133*(5), 184.

[43] Raja, M. A. Z., Shah, Z., Manzar, M. A., Ahmad, I., Awais, M., & Baleanu, D. (2018). A new stochastic computing paradigm for nonlinear Painlevé II systems in applications of random matrix theory. *The European Physical Journal Plus*, *133*(7), 254.

[44] Raja, M. A. Z., Shah, F. H., Khan, A. A., & Khan, N. A. (2016). Design of bio-inspired computational intelligence technique for solving steady thin film flow of Johnson–Segalman fluid on vertical cylinder for drainage problems. *Journal of the Taiwan Institute of Chemical Engineers*, *60*, 59-75.

[45] Ahmad, I., et al., 2019. Design of computational intelligent procedure for thermal analysis of porous fin model. *Chinese Journal of Physics*, *59*, pp.641-655.

[46] Mehmood, A., et al., (2018). Parameter estimation for Hammerstein control autoregressive systems using differential evolution. *Signal, Image and Video Processing*, 12(8), 1603-1610.

[47] Raja, M. A. Z., Shah, A. A., Mehmood, A., Chaudhary, N. I., & Aslam, M. S. (2018). Bio-inspired computational heuristics for parameter estimation of nonlinear Hammerstein controlled autoregressive system. *Neural Computing and Applications*, *29*(12), 1455-1474.

[48] Khan, W. U., et al., (2018). Backtracking search integrated with sequential quadratic programing for nonlinear active noise control systems. *Applied Soft Computing*, *73,* 666-683.

[49] Khan, W.U., et al., 2019. A novel application of fireworks heuristic paradigms for reliable treatment of nonlinear active noise control. *Applied Acoustics*, *146*, pp.246-260.

[50] Mehmood, A., et al., (2019). Nature-inspired heuristic paradigms for parameter estimation of control autoregressive moving average systems. *Neural Computing and Applications*, *31*(10), 5819-5842.

[51] Ahmad, I., et al., (2016). Bio-inspired computational heuristics to study Lane–Emden systems arising in astrophysics model. *SpringerPlus*, *5*(1), 1866.

[52] Pathak, M., & Joshi, P. (2018). Application of a coupled approach for the solution of nonlinear singular initial value problems of Lane–Emden type. *Astrophysics and Space Science*, *363*(9), 191.

[53] Raja, M. A. Z., Zameer, A., Khan, A. U., & Wazwaz, A. M. (2016). A new numerical approach to solve Thomas–Fermi model of an atom using bio-inspired heuristics integrated with sequential quadratic programming. *SpringerPlus*, *5*(1), 1400.

[54] Sabir, Z., et al., (2018). Neuro-heuristics for nonlinear singular Thomas-Fermi systems. *Applied Soft Computing*, *65*, 152-169.

[55] Raja, M. A. Z., Shah, F. H., Tariq, M., & Ahmad, I. (2018). Design of artificial neural network models optimized with sequential quadratic programming to study the dynamics of nonlinear Troesch's problem arising in plasma physics. *Neural Computing and Applications*, *29*(6), 83-109.

[56] Majeed, K., et al., (2017). A genetic algorithm optimized Morlet wavelet artificial neural network to study the dynamics of nonlinear Troesch's system. *Applied Soft Computing*, *56*, 420-435.

[57] Ahmad, I., et al., (2017). Neural network methods to solve the Lane–Emden type equations arising in thermodynamic studies of the spherical gas cloud model. *Neural Computing and Applications*, *28*(1), 929-944.

[58] Raja, M. A. Z., Niazi, S. A., & Butt, S. A. (2017). An intelligent computing technique to analyze the vibrational dynamics of rotating electrical machine. *Neurocomputing*, *219*, 280-299.

[59] Vitayasak, S., & Pongcharoen, P. (2018). Performance improvement of Teaching-Learning-Based Optimisation for robust machine layout design. *Expert Systems with Applications*, *98*, 129-152.

[60] Mehmood, A., et al., 2018. Design of neuro-computing paradigms for nonlinear nanofluidic systems of MHD Jeffery–Hamel flow. *Journal of the Taiwan Institute of Chemical Engineers*, *91*, pp.57-85.

[61] Raja, M. A. Z., Ahmed, T., & Shah, S. M. (2017). Intelligent computing strategy to analyze the dynamics of convective heat transfer in MHD slip flow over stretching surface involving carbon nanotubes. *Journal of the Taiwan Institute of Chemical Engineers*, *80*, 935-953.

[62] Mehmood, A., et al., Design of nature-inspired heuristic paradigm for systems in nonlinear electrical circuits. *Neural Computing and Applications*, pp.1-17.

[63] Raja, M. A. Z., Mehmood, A., Niazi, S. A., & Shah, S. M. 2018. Computational intelligence methodology for the analysis of RC circuit modelled with nonlinear differential order system. *Neural Computing and Applications*, *30*(6), pp. 1905–1924.

[64] Li, Y. Z., Jiang, L., Wu, Q. H., Wang, P., Gooi, H. B., Li, K. C., ... & Imura, J. (2017). Wind-thermal power system dispatch using MLSAD model and GSOICLW algorithm. *Knowledge-Based Systems*, *116*, 94-101.

[65] Nuaekaew, K., Artrit, P., Pholdee, N., & Bureerat, S. (2017). Optimal reactive power dispatch problem using a two-archive multi-objective grey wolf optimizer. *Expert Systems with Applications*, *87*, 79-89.

[66] Mehmood, A., et al., Novel computing paradigms for parameter estimation in power signal models. *Neural Computing and Applications*, pp.1-30.

[67] Zameer, A., et al., (2017). Intelligent and robust prediction of short term wind power using genetic programming based ensemble of neural networks. *Energy conversion and management*, *134*, 361-372.

[68] Kelly, S., & Ahmad, K. (2018). Estimating the impact of domain-specific news sentiment on financial assets. *Knowledge-Based Systems*, *150*, 116-126.

[69] Ara, A., et al., 2018. Wavelets optimization method for evaluation of fractional partial differential equations: an application to financial modelling. *Advances in Difference Equations*, *2018*(1), p.8.

[70] Karhunen, M. (2019). Algorithmic sign prediction and covariate selection across eleven international stock markets. *Expert Systems with Applications*, *115*, 256-263.

[71] Cerqueti, R., Ferraro, G., & Iovanella, A. (2018). A new measure for community structures through indirect social connections. *Expert Systems with Applications*, *114*, 196-209.

[72] Raja, M. A. Z., Asma, K., & Aslam, M. S. (2018). Bio-inspired computational heuristics to study models of hiv infection of CD4+ T-cell. *International Journal of Biomathematics*, *11*(02), 1850019.

[73] Raja, M. A. Z., Shah, F. H., Alaidarous, E. S., & Syam, M. I. (2017). Design of bio-inspired heuristic technique integrated with interior-point algorithm to analyze the dynamics of heartbeat model. *Applied Soft Computing*, *52*, 605-629.

[74] Storn, R., & Price, K. (1997). Differential evolution–a simple and efficient heuristic for global optimization over continuous spaces. *Journal of global optimization*, *11*(4), 341-359.

[75] Price, K., Storn, R. M., & Lampinen, J. A. (2006). *Differential evolution: a practical approach to global optimization*. Springer Science & Business Media.

[76] Buba, A. T., & Lee, L. S. (2018). A differential evolution for simultaneous transit network design and frequency setting problem. *Expert Systems with Applications*, *106*, 277-289.

[77] Mlakar, U., Fister, I., Brest, J., & Potočnik, B. (2017). Multi-objective differential evolution for feature selection in facial expression recognition systems. *Expert Systems with Applications*, *89*, 129-137.

[78] Li, H., Gong, M., Wang, C., & Miao, Q. (2018). Self-paced stacked denoising autoencoders based on differential evolution for change detection. *Applied Soft Computing*, *71*, 698-714.

[79] Sayah, S. (2018). Modified differential evolution approach for practical optimal reactive power dispatch of hybrid AC− DC power systems. *Applied Soft Computing*.

[80] Vali, M. H., Aghagolzadeh, A., & Baleghi, Y. (2018). Optimized watermarking technique using self-adaptive differential evolution based on redundant discrete wavelet transform and singular value decomposition. *Expert Systems with Applications*, *114*, 296-312.

[81] Hancer, E., Xue, B., & Zhang, M. (2018). Differential evolution for filter feature selection based on information theory and feature ranking. *Knowledge-Based Systems*, *140*, 103-119.

[82] Holland, J. H. (1992). Genetic algorithms. *Scientific american*, *267*(1), 66-73.

[83] Davis, L. (1991). Handbook of genetic algorithms.

[84] Keshavarz, H., & Abadeh, M. S. (2017). ALGA: Adaptive lexicon learning using genetic algorithm for sentiment analysis of microblogs. *Knowledge-Based Systems*, *122*, 1-16.

[85] Raman, M. G., Somu, N., Kirthivasan, K., Liscano, R., & Sriram, V. S. (2017). An efficient intrusion detection system based on hypergraph-Genetic algorithm for parameter optimization and feature selection in support vector machine. *Knowledge-Based Systems*, *134*, 1-12.

[86] Tseng, H. E., Chang, C. C., Lee, S. C., & Huang, Y. M. (2018). A Block-based genetic algorithm for disassembly sequence planning. *Expert Systems with Applications*, *96*, 492-505.

[87] Owais, M., & Osman, M. K. (2018). Complete hierarchical multi-objective genetic algorithm for transit network design problem. *Expert Systems with Applications*, *114*, 143-154.

[88] Jadhav, S., He, H., & Jenkins, K. (2018). Information gain directed genetic algorithm wrapper feature selection for credit rating. *Applied Soft Computing*, *69*, 541-553.

[89] Raja, M. A. Z., Mehmood, A., ur Rehman, A., Khan, A., & Zameer, A. (2018). Bio-inspired computational heuristics for Sisko fluid flow and heat transfer models. *Applied Soft Computing*, *71*, 622-648.

[90] Chouhdry, Z.R., et al., 2018. Design of reduced search space strategy based on integration of Nelder–Mead method and pattern search algorithm with application to economic load dispatch problem. *Neural Computing and Applications*, *30*(12), pp.3693-3705.

[91] Raja, M.A.Z. and Samar, R., 2014. Solution of the 2-dimensional Bratu problem using neural network, swarm intelligence and sequential quadratic programming. *Neural Computing and applications*, *25*(7-8), pp.1723-1739.

[92] Raja, M.A.Z., Khan, J.A. and Qureshi, I.M., 2010. A new stochastic approach for solution of Riccati differential equation of fractional order. *Annals of Mathematics and Artificial Intelligence*, *60*(3-4), pp.229-250.